Accepted Manuscript

Ocean circulation and freshwater pathways in the Arctic Mediterranean based on a combined Nd isotope, REE and oxygen isotope section across Fram Strait

Georgi Laukert, Martin Frank, Dorothea Bauch, Ed C. Hathorne, Benjamin Rabe, Wilken-Jon von Appen, Carolyn Wegner, Moritz Zieringer, Heidemarie Kassens
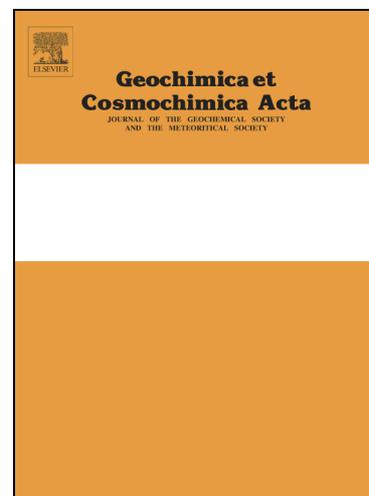
Please cite this article as: Laukert, G., Frank, M., Bauch, D., Hathorne, E.C., Rabe, B., von Appen, W-J., Wegner, C., Zieringer, M., Kassens, H., Ocean circulation and freshwater pathways in the Arctic Mediterranean based on a combined Nd isotope, REE and oxygen isotope section across Fram Strait, *Geochimica et Cosmochimica Acta* (2016), doi: http://dx.doi.org/10.1016/j.gca.2016.12.028

Ocean circulation and freshwater pathways in the Arctic Mediterranean based on a combined Nd isotope, REE and oxygen isotope section across Fram Strait

Georgi Laukert [a,*], Martin Frank [a], Dorothea Bauch [a], Ed C. Hathorne [a], Benjamin Rabe [b], Wilken-Jon von Appen [b], Carolyn Wegner [a], Moritz Zieringer [a], Heidemarie Kassens [a]

[a] GEOMAR Helmholtz Centre for Ocean Research Kiel, Wischhofstr. 1-3, 24148 Kiel, Germany

[b] Alfred Wegener Institute, Helmholtz Centre for Polar and Marine Research, Am Handelshafen 12, 27570 Bremerhaven, Germany

* Corresponding author at: GEOMAR Helmholtz Centre for Ocean Research Kiel, Wischhofstr. 1-3, 24148 Kiel, Germany. Tel.: +49 431 600 2888. E-mail address: glaukert@geomar.de.

1

ABSTRACT

The water masses passing the Fram Strait are mainly responsible for the exchange of heat and freshwater between the Nordic Seas and the Arctic Ocean (the Arctic Mediterranean, AM). Disentangling their exact sources, distribution and mixing, however, is complex. This work provides new insights based on a detailed geochemical tracer inventory including dissolved Nd isotope (ε_{Nd}), rare earth element (REE) and stable oxygen isotope ($\delta^{18}O$) data along a full water depth section across Fram Strait.

We find that Nd isotope and REE distributions in the open AM primarily reflect lateral advection of water masses and their mixing. Seawater-particle interactions exert important control only above the shelf regions, as observed above the NE Greenland Shelf. Advection of northward flowing warm Atlantic Water (AW) is clearly reflected by an ε_{Nd} signature of -11.7 and a Nd concentration ([Nd]) of 16 pmol/kg in the upper ~500 m of the eastern and central Fram Strait. Freshening and cooling of the AW on its way trough the AM are accompanied by a continuous change towards more radiogenic ε_{Nd} signatures (e.g. -10.4 of dense Arctic Atlantic Water). This mainly reflects mixing with intermediate waters but also admixture of dense Kara Sea waters and Pacific-derived waters. The more radiogenic ε_{Nd} signatures of the intermediate and deep waters (reaching -9.5) are mainly acquired in the SW Nordic Seas through exchange with basaltic formations of Iceland and SE Greenland. Inputs of Nd from Svalbard are not observed and surface waters and Nd on the Svalbard shelf originate from the Barents Sea. Shallow southward flowing Arctic-derived waters (< 200 m) form the core of the East Greenland Current above the Greenland slope and can be traced by their relatively radiogenic ε_{Nd} (reaching -8.8) and elevated [Nd] (21 to 29 pmol/kg). These properties are used together with $\delta^{18}O$ and standard hydrographic tracers to define the proportions of Pacific-derived (< ~30 % based on Nd isotopes) and Atlantic-derived waters, as well as of river waters (< ~8 %). Shallow waters (< 150 m) on the NE Greenland Shelf share some characteristics of Arctic-derived waters, but exhibit less radiogenic ε_{Nd} values (reaching -12.4)

2

and higher [Nd] (up to 38 pmol/kg) in the upper ~100 m. This suggests local addition of

Greenland freshwater of up to ~6 %. In addition to these observations, this study shows that

the pronounced gradients in ε_{Nd} signatures and REE characteristics in the upper water column

provide a reliable basis for assessments of shallow hydrological changes within the AM.

1. INTRODUCTION

The oceanic heat and freshwater budget of the Arctic Mediterranean (i.e. the Arctic Ocean

and Nordic Seas, AM) is highly sensitive to climate forcing and in turn has a major impact on

global climate variability (cf. Anisimov et al., 2007). A thorough assessment of sources,

distribution and circulation of water masses involved in the transport and transfer of heat and

freshwater within the AM is therefore critical for our understanding of present and potential

future hydrological changes in the high-latitude and polar regions.

Together with the shallow Barents Sea (average depth of ~230 m), the deep (sill depth

of 2545 m) and wide (~500 km) Fram Strait acts as a fundamental gateway through which

water masses, and therefore heat and freshwater, exchange between the Arctic Ocean (AO)

and the Nordic Seas (NS). Mixing processes upstream, downstream and within the Strait thus

exert significant influence on climate (e.g. Aagaard et al., 1985; Rudels, 2009). Warm and

saline Atlantic-derived waters, cold and fresh Arctic-derived waters and intermediate and

deep waters from the AM deep basins meet and interact in the Fram Strait (e.g. Rudels et al.,

1999b), which results in a complex hydrography involving a large number of distinct water

masses that have been tracked by their temperature, salinity and potential density

characteristics (e.g. Rudels et al., 2005; Schlichtholz and Houssais, 2002). Enhanced melting

of the Greenland ice sheet additionally affects the upper water column of the western Fram

Strait through increasing admixture of Greenland freshwater (e.g. Stedmon et al., 2015). The

fate of the latter in the NS and its potential influence on the circulation pathways is not well

3

known, which emphasizes the demand of a detailed geochemical inventory of water masses in this region.

Assessments of the fractional contributions to Arctic water masses have been carried out in previous studies but results based on different methodologies show significant discrepancies, in particular with regard to the contribution of Pacific-derived waters (Alkire et al., 2015). Here we use a novel combination of dissolved neodymium (Nd) isotope, rare earth element (REE) and stable oxygen isotope (δ^{18}O) measurements with standard hydrographic tracers (T, S, NO_3, PO_4, Si) to refine the characterization of water masses along a zonal section crossing Fram Strait between Svalbard and Greenland, including the shallow North-East (NE) Greenland Shelf. The combination of standard hydrographic properties and δ^{18}O allows distinguishing between meteoric waters, sea-ice meltwater and Atlantic-derived and Pacific-derived waters within the Arctic halocline (e.g. Ekwurzel et al., 2001; Jones et al., 2008a; Jones et al., 1998; Newton et al., 2013; Yamamoto-Kawai et al., 2008). The fractions of these waters have previously been determined for waters in the Fram Strait region and further south applying different sets of mass balance calculations and end-members (e.g. de Steur et al., 2015; Dodd et al., 2009; Dodd et al., 2012; Falck, 2001; Falck et al., 2005; Jones et al., 2008b; Rabe et al., 2013; Stedmon et al., 2015; Sutherland et al., 2009; Taylor et al., 2003). However, besides the uncertainties mentioned above, these assessments lack a distinction of the different meteoric waters and their sources. Here radiogenic Nd isotopes provide important information given that water masses acquire their dissolved signatures mainly through particulate and dissolved riverine inputs of weathered continental crustal material, as well as exchange with the ocean margin sediments (Lacan and Jeandel, 2001, 2005), for which the Nd isotopic compositions vary as a function of the age and the Sm/Nd ratio of the source rocks (Frank, 2002). The quasi-conservative behavior of Nd in the open ocean (Frank, 2002; Goldstein and Hemming, 2003) and its intermediate average oceanic residence time of several hundred years (Arsouze et al., 2009; Rempfer et al., 2011;

4

Tachikawa et al., 2003) then allows the tracking of these water masses and their mixing in the open ocean. The dissolved REE concentrations and their relative distribution patterns provide complementary information on the composition of the source material, the amount of time since the last contact with weathering inputs, and adsorption and desorption processes (e.g. Garcia-Solsona et al., 2014; Haley et al., 2014; Hathorne et al., 2015; Molina-Kescher et al., 2014). This is possible because of systematic changes in the particle-reactivity of the REEs across the group caused by decreasing ionic radii and increasing covalent character with increasing atomic number.

The combination of dissolved Nd isotope compositions, REE distributions, $\delta^{18}O$ and hydrographic properties in the Fram Strait applied in this study for the first time allows a detailed evaluation of the suitability of Nd isotopes as water mass tracer in the AM and an assessment of the origin and mixing of water masses in the AM based on geochemical properties.

2. ARCTIC MEDITERRANEAN REE AND ND ISOTOPE CHARACTERISTICS

Figure 1a shows the major potential REE sources and their Nd isotopic compositions (i.e. the radiogenic Nd isotope ratio $^{143}Nd/^{144}Nd$, commonly expressed as ε_{Nd} = $[(^{143}Nd/^{144}Nd)_{sample}/(^{143}Nd/^{144}Nd)_{CHUR} -1] \times 10^4$ with CHUR = 0.512638 and referring to a 'CHondritic Uniform Reservoir'; Jacobsen and Wasserburg, 1980) in the AM based on previously reported and new data from this study. Atlantic Water (AW) that enters the AM is characterized by an average ε_{Nd} signature of -13.0 (1 SD = 0.6, n = 7) and -12.6 (1 SD = 0.8, n = 2) and an average Nd concentration ([Nd]) of 16.2 and 19.1 pmol/kg (1 SD = 2.1 and 0.5, respectively) at the Iceland-Scotland Ridge and the Denmark Strait, respectively (data from Lacan and Jeandel, 2004a, 2004b). The Pacific-derived waters entering the AO through the Bering Strait have ε_{Nd} values between -4 and -6 (Dahlqvist et al., 2007). These waters are likely modified towards less radiogenic compositions through water-shelf interaction in the

5

Chukchi Sea, which results in ε_{Nd} values of $\sim$ -5.5 and Nd concentrations of up to $\sim$30 pmol/kg for waters leaving the shelf (PACW; Porcelli et al., 2009). The Norwegian Coastal Water (NCW) is another marine REE source that originates from the Baltic Sea (Gascard et al., 2004) and enters the AM from the North Sea flowing along the western and northern coast of Norway into the Barents Sea (Loeng, 1991). In the western Barents Sea it is characterized by ε_{Nd} = -14.5 and [Nd] = 22.5 pmol/kg (Petrova, 2015) consistent with its Baltic Sea origin (i.e. ε_{Nd} = -15.6 close to the Danish Straits, Chen et al., 2013). The Siberian and North American Rivers draining into the AO have a wide range of Nd concentrations and isotopic compositions (Persson et al., 2011; Porcelli et al., 2009; Zimmermann et al., 2009). Their initial Nd concentrations can be 100 times higher than those of typical seawater, but a considerable fraction is removed in estuaries and on the Arctic shelves (Porcelli et al., 2009), preventing most of the riverine Nd to reach the open AO. The potential for additional input of REEs and/or modification of the Nd isotopic composition through other weathering sources and processes, including release from particles and sediments, sea-ice formation and melting, glacial meltwater/runoff, and eolian dust remains to be investigated in detail.

The seawater Nd isotope distribution in the AM has been attributed to weathering inputs, water mass circulation and mixing, but also to seawater-sediment exchange processes occurring on the wide Siberian shelves and the shelf slopes (e.g. Andersson et al., 2008; Porcelli et al., 2009). The unknown impact of the latter and the scarcity of Nd data available so far prevented exploring the full potential of Nd isotopes as a water mass tracer in the AM. Moreover, the majority of the previous studies focusing on the distribution of Nd isotopes only reported the concentrations of Nd (Andersson et al., 2008; Lacan and Jeandel, 2004a; Piepgras and Wasserburg, 1987; Porcelli et al., 2009; Werner et al., 2014; Zimmermann et al., 2009). Despite their potential as a source tracer, there are only two studies that so far reported distributions of all REEs for unfiltered seawater in the AM (Lacan and Jeandel, 2004b;

6

Westerlund and Ohman, 1992), and one providing dissolved REEs for the Canada Basin (Yang and Haley, 2016).

3. METHODS

3.1 General information and oceanographic data

All samples presented in this study were acquired during the first leg of the 27th expedition of the German research vessel FS Polarstern between 15 June and 15 July 2012 (PS80, ARKXXVII/1). Details about the cruise track, sea-ice conditions and other information can be found in the expedition report (Beszczynska-Möller, 2013).

CTD (conductivity, temperature, depth) profiles were obtained along a latitudinal transect between 9.3° E and 12.5° W at approximately 78.8° N and on the NE Greenland Shelf along the fast ice edge, between 78.5° N and 79.8° N (Fig. 1b; Beszczynska-Möller and Wisotzki, 2012). Seawater samples were collected along the meridional section at 78.8° N covering the entire Fram Strait and continuing on the NE Greenland Shelf in the inter-trough area east of the Northwind Shoal. A SBE32 rosette water sampler equipped with 24 Niskin-type sample bottles (12 L) was used for recovery of all samples. Samples for Nd isotope and REE analyses were recovered from the full water column of the central Fram Strait down to a maximum depth of 2668 m, while the sampling depth on the NE Greenland Shelf and the western Svalbard Shelf reached 395 and 197 m, respectively. Samples for oxygen isotope and nutrient analyses were taken at different stations and depths along the cruise track due to limited sampling time and capabilities onboard, but the geographical distribution of these stations fully cover the distribution of the Nd and REE stations with maximum meridional and zonal distances between the data points of less than ~10 km and ~14 km, respectively. Sampling locations for all parameters are shown in Fig. 1b.

In addition, we report the Nd isotopic composition and concentration of one sample from the Laptev Sea margin (~200 m depth) and one surface sample from the SE Laptev Sea

close to the Lena River delta acquired during the Transdrift-22 (September 2014) and Transdrift-21 (September 2013) expeditions, respectively.

3.2 Nd isotopic composition, $[Nd]_{ID}$ and [REE]

The entire pre-concentration, purification and measurement techniques reported here strictly followed approved GEOTRACES protocols and were confirmed through participation in the international GEOTRACES inter-calibration study (van de Flierdt et al., 2012). Samples for Nd isotopic analyses were collected in 20 L (Fram Strait samples) or 10 L (Laptev Sea samples) acid-cleaned LDPE-cubitainers and immediately filtered through 0.45 μm Millipore® cellulose acetate filters using a peristaltic pump (Fram Strait samples) or through AcroPak™500 Capsules with Supor Membrane (pore size: 0.8/0.2 μm) filter cartridges (Laptev Sea samples) and subsequently acidified to pH ~2.2 with ultra-pure concentrated hydrochloric acid within 2 hours after sampling (Fram Strait samples) or after transport to the Otto-Schmidt Laboratory in St. Petersburg, Russia (Laptev Sea samples). An aliquot of 2 L of each sample was separated into an acid-cleaned LDPE-bottle for concentration analyses. About ~100 mg of Fe was added to the remaining large sample as purified $FeCl_3$ solution (~1 g $Fe(III)Cl_3$/mL) and at least 48 hours for equilibration was given before the pH was adjusted to ~8 using ammonia solution (25%, Merck Suprapur®) leading to co-precipitation of the dissolved REEs together with the iron hydroxides (FeOOH). Most of the supernatant was discarded and the Fe-precipitate transferred into a 2 L acid-cleaned LDPE-bottle and returned to the home laboratory at GEOMAR, Kiel.

For the extraction and isolation of dissolved Nd a procedure similar to that described by Stichel et al. (2012) was applied: The Fe-precipitates were centrifuged and rinsed with deionized (18.2 MΩ cm, Milli-Q system) water to remove major seawater ions. Organic components were then destroyed by treatment with concentrated aqua regia (heated for at least 24 h at 110°C). Afterwards, clean diethyl ether was used to separate Fe from the samples

8

(liquid-liquid extraction). Major element cations were separated from the REEs through cation exchange chromatography (BIORAD® AG50W-X8 resin, 200-400 μm mesh-size, 1.4 mL resin bed) with a slightly modified separation scheme of Stichel et al. (2012), where instead of a mixture of HCl and HF acids only HCl was used as a reagent. Neodymium separation from the other REEs was achieved by a second column chemistry step using Eichchrom® Ln Spec resin (50-100 μm mesh size, 2 mL resin bed) and the separation scheme from Le Fèvre and Pin (2005). Nd concentrations ([Nd]) were determined using an isotope dilution (ID) method (i.e. $[Nd]_{ID}$) after Rickli et al. (2009). A pre-weighed ^{150}Nd spike was added to a 0.5 L aliquot of each sample and after equilibration and addition of Fe-hydroxide co-precipitation was achieved at pH ~8. For REE separation the same method as for the isotope measurements was used but only the cation exchange chromatography was applied.

Neodymium isotope compositions and $[Nd]_{ID}$ were measured on a Nu plasma MC-ICP-MS at GEOMAR, Kiel. An exponential mass fractionation law was applied for correction of instrumental mass bias using a $^{146}Nd/^{144}Nd$ ratio of 0.7219. The measured $^{143}Nd/^{144}Nd$ ratios of all samples were normalized to the value of 0.512115 for the JNdi-1 standard (Tanaka et al., 2000). Based on repeated measurements (every two samples) of JNdi-1 and in-house standards with concentrations similar to those of the samples, the 2σ external reproducibility ranged between 0.2 and 0.3 ε_{Nd} units for the individual measurement runs. Duplicate analyses (n = 10) resulted in identical Nd isotopic compositions within these uncertainties. Replicates of the isotope dilution measurements (n = 13) yielded an external reproducibility of 1.5 % (2σ) on average.

REE concentrations were measured using an online pre-concentration (OP) ICP-MS technique at GEOMAR, Kiel by directly coupling a "seaFAST" system (Elemental Scientific Inc., Nebraska, USA) to an ICP-MS (Agilent 7500ce) (Hathorne et al., 2012). The method of Hathorne et al. (2012) was further improved by using 8 mL sample loop and by preparation of calibration standards with a mixed REE solution of a seawater-like composition in a natural

seawater matrix (Osborne et al., 2015). Trace metals including REEs were quantitatively removed from the seawater matrix through FeOOH co-precipitation yielding REE concentrations (generally < 0.2 pmol/kg for Ce and lower for all other REEs) in the resulting emptied seawater indistinguishable from distilled 0.1 % HCl. Repeated measurements of GEOTRACES inter-calibration samples BATS 15 m and BATS 2000 m from the Bermuda Atlantic Time-Series (van de Flierdt et al., 2012) were used to monitor the external reproducibility (electronic supplement B).

3.3 Oxygen isotopes and nutrient analyses

For oxygen isotope analyses a CO_2-water isotope equilibration technique n (Epstein and Mayeda, 1953) on a Finnigan gas bench II unit coupled to a Finnigan DeltaPlusXL was applied to at least two subsamples of the same water sample at the Leibniz Laboratory for Radiometric Dating and Stable Isotope Research, Kiel. The external reproducibility for all $\delta^{18}O$ measurements is ±0.04 ‰ or smaller and the measured $^{18}O/^{16}O$ ratio is provided as a deviation from Vienna Standard Mean Ocean Water in the δ-notation (Craig, 1961).

Nutrient samples were collected in plastic bottles and directly frozen at -80 °C and stored at -20 °C. Silicate, phosphate, nitrate and nitrite were analyzed at GEOMAR Helmholtz Centre for Ocean Research Kiel following standard procedures (Grasshoff et al., 2009).

3.4 Water mass classification, PO* and N/P methods and Nd-based mixing

We assigned water masses to most samples presented in this study and literature Nd data from the entire AM based on the classification of Rudels et al. (2012; 2005). This classification is based on constant θ-S end-member definitions and therefore does not take into account changes in the end-member properties, such as the warming of deep-water masses observed at Fram Strait over the last two decades (von Appen et al., 2015). To address the latter

10

observation at least in a way that prevents misinterpretation, we do not distinguish between Eurasian Basin Deep Water and Greenland Sea Deep Water. The classification also broadly defines waters with $\sigma_\theta < {\sim}27.7$ as Polar Surface Water (PSW), thus not considering studies that pointed to contributions of locally formed waters on the NE Greenland Shelf (Bignami and Hopkins, 1997; Budéus and Schneider, 1995; Budéus et al., 1997). Consequently, for waters with $\sigma_\theta < {\sim}27.7$, we instead combine findings of Bignami and Hopkins (1997) and Budéus et al. (1997) and ascribe particular recurring θ-S properties and silicate concentrations to distinct water masses. We refer to these water masses as NE Greenland Shelf Shallow Water (NEGSSW, $S \leq {\sim}31.8$) and NE Greenland Shelf Bottom Water (NEGSBW, $S \sim 34.4$), as well as silicate-rich Polar Water (PW, [Si] > ~6 to ~8 μmol/kg, $\sim 32 < S < {\sim}33.5$) and silicate-poor Knee Water (KW, [Si] < ~5 μmol/kg, $S \sim 34$, T near freezing point).

For shallow samples recovered from the western Fram Strait (i.e. mostly NEGSSW, NEGSBW, PW or KW), fractions of the source-defined components (i.e. meteoric water, MW, sea-ice meltwater, SIM, Atlantic-derived water, ATL, and Pacific-derived water, PAC) were calculated based on different empirical nutrient ratios (referred to as N/P method) and a phosphate-oxygen relationship (referred to as PO* method) following Bauch et al. (2011), who also provide the end-member compositions. Due to insignificantly small quantities of PAC combined with the inaccuracies in end-members and measurements, some of the calculated PAC fractions may be negative and have no physical meaning. In these cases, a three-component system of equations is applied instead and the fraction of PAC set to zero. For mixing between Arctic-derived waters and Greenland freshwater, the interpolated $\delta^{18}O$ value (-1.5 ‰) of the PW sample with the most radiogenic ε_{Nd} signature was used as the marine $\delta^{18}O$ end-member, while for salinity, [Nd] and Nd isotopes the average composition of PW was used to account for modification of this water mass on the NE Greenland Shelf. For the Greenland freshwater end-member, the $\delta^{18}O$ was set to -23.4 ‰ (Stedmon et al., 2015).

Two-component mixing based on S, [Nd] and Nd isotopes was calculated following

11

$$\varepsilon Nd_{MIX} = \frac{\varepsilon Nd_1 * [Nd]_1 * S_1 * f_1 + \varepsilon Nd_2 * [Nd]_2 * S_2 * f_2}{[Nd]_1 * S_1 * f_1 + * [Nd]_2 * S_2 * f_2}$$

and

$$1 = f_1 + f_2$$

where f_1 and f_2 denote the mass fractions of end-member 1 and 2, respectively, and εNd_{MIX} is the ε_{Nd} value of the mixture of the two end-members. Note that we do not use an optimum multiparameter analysis here due to the poorly defined end-member compositions of most of the water masses of the AM. In addition, significant seasonal and interannual variations of the upper water column and longer term changes in hydrographic properties of the intermediate and deep waters render such a steady-state approach unsuitable in the study area.

4. RESULTS

All CTD data including temperature, salinity, oxygen concentration, O_2-saturation and attenuation were reported previously by Beszczynska-Möller and Wisotzki (2012) and are available through the PANGEA database (https://doi.pangaea.de/10.1594/PANGAEA.801791). Neodymium isotopic compositions, [Nd] obtained from the isotope dilution method, and REE concentrations measured with OP-ICP-MS are reported in the electronic supplement B together with corresponding S, T, O_2 concentrations and attenuation. Nutrient concentrations and $\delta^{18}O$ values are reported in the same way. All data are in addition accessible through the PANGEA database. The average Nd isotope and REE characteristics of all water masses resulting from our study are also listed in table 1 together with salinity and are reported in electronic supplement A in more detail, where also a compilation of the composition of all water masses of the AM is provided.

12

4.1 Hydrography, water mass distribution and water mass components

The θ-S distribution of the waters of our study is presented in Fig. 2 (black dots) and is within the typical θ-S range at Fram Strait and the NE Greenland Shelf (e.g. Budéus et al., 1997; Schlichtholz and Houssais, 2002). Waters confined to the NE Greenland Shelf and the upper water column (~300 m) above the Greenland continental margin (density $\sigma_\theta < \sim 27.7$) exhibit recurring θ-S features (i.e. the sharp inflection at S ~34 and data tightly clustering at S ~31.8 before showing a larger scatter at lower salinities) and salinities reaching values as low as ~30. In contrast, the waters occupying most of the Fram Strait section ($\sigma_\theta > \sim 27.7$, including AW, intermediate and deep waters, insets A and B in Fig. 2) show only limited variations in S, but a pronounced increase in temperatures towards the surface.

The distribution of water masses in 2012 overall matches earlier observations very well (e.g. Rudels et al., 2000). As shown in Fig. 3, the main core of AW is located shallower than ~500 m depth at the eastern side of Fram Strait and exhibits $S_{max} = 35.14$ and $T_{max} = 5.36$ °C in 2012. The AW comprises surface and intermediate waters that are transported northward into the AO along the Svalbard continental margin via the West Spitsbergen Current (WSC; e.g. Rudels et al., 2004), which is the northernmost extension of the Norwegian Atlantic Current (NAC; Aagaard et al., 1987) (Fig. 1). The surface front between inflowing AW that has never interacted with sea ice and the outflowing PSW is located near the Greenwich meridian. Patches of Recirculating Atlantic Water (RAW), which return to the NS within the Fram Strait or slightly north of it, are found near the front in the western Fram Strait below the surface. All water masses constituting PSW are located in the upper water column (~300 m) between this front and the coast of Greenland, with PW and KW forming the core of the EGC and NEGSSW and NEGSBW occupying the water column west of the EGC on the NE Greenland Shelf. Below RAW, dense Arctic Atlantic Water (dAAW) is found in the western Fram Strait at depths of ~400 to ~900 m. According to the θ-S-based classification, Arctic Intermediate Water (AIW) prevails below the AW/RAW/dAAW layer

13

on both sides of Fram Strait, while Upper Polar Deep Water (UPDW) is mainly distributed

above the continental slope of Greenland. Similarly, Eurasian Basin Deep Water (EBDW) or

Greenland Sea Deep Water (GSDW) and Canada Basin Deep Water (CBDW) prevail on both

sides of Fram Strait, while Nordic Seas Deep Water (NDW) is mostly confined to the

Svalbard continental slope. For further information on the water mass distribution and

characteristics in 2012, as well as the long-term variability, the reader is referred to

Beszczynska-Möller (2013).

Similar fractions of MW (f_{MW}) and SIM (f_{SIM}) were computed with the PO* and N/P

methods for PSW (the N/P based distributions are shown in Fig. 4), with the values of f_{MW}

calculated with the PO* approach being somewhat higher compared to the N/P-based values

(up to ~2 %) as a response to different consideration of marine fractions. Discrepancies to a

far greater extent (up to ~40 %) are observed for the fractions of PAC (f_{PAC}) and ATL (f_{ATL})

between both methods, with the N/P method computing higher f_{PAC} and thus lower f_{ATL}

compared to the PO* method (Fig. 4). A Monte Carlo approach applied by Alkire et al.

(2015) to examine uncertainties in the different fractions yields median standard deviations

for f_{MW}, f_{SIM} and f_{PAC} of 1%, 0.6% and 13%, respectively, outlining the high uncertainties of

the calculated fractions of PAC. Therefore, we adopt f_{MW} and f_{SIM} from the PO* and N/P

methods, but show f_{PAC} of both methods for comparison with Nd-based estimates only.

4.2 Nd isotopes, [Nd]$_{ID}$ and [REE]

The Nd isotope and REE data set obtained covers the entire θ-S-range of the CTD data and

includes all water masses present (Fig. 2). Neodymium concentrations obtained by isotope

dilution range between 14.8 and 38.1 pmol/kg (Figs. 3 and 4), with lowest and highest [Nd]$_{ID}$

values observed above the western Svalbard Shelf and the NE Greenland Shelf, respectively.

Waters with σ_θ > ~27.7 show only limited variations in [Nd]$_{ID}$ (average = 15.9 pmol/kg, 1 SD

= 0.7, n = 58), while waters with σ_θ < ~27.7 show an inverse gradient with highest [Nd]$_{ID}$

14

values observed for NEGSSW. Two samples (station 68, 15.3 m; station 132, 202.6 m) exhibited anomalously high $[Nd]_{ID}$ (38.1 pmol/kg and 27.0 pmol/kg, respectively), neither consistent with Nd concentrations of adjacent samples nor with oceanographic properties. The REE patterns of these samples indicate that only the light REEs are anomalously enriched. Since we cannot completely rule out contamination during sampling, we report the $[Nd]_{ID}$ values of these two samples but exclude them from the figures and the following discussion.

Neodymium concentrations obtained by OP-ICP-MS are identical to the $[Nd]_{ID}$ data within the 95 % confidence limits of the OP-ICP-MS technique (see Hathorne et al., 2012 for more details), with the maximum difference between the two methods being ~15 % (sample 130-200). Similar to $[Nd]_{ID}$, all REE and Y concentrations are nearly constant throughout the whole water column for waters with $\sigma_\theta > \sim 27.7$, in agreement with unfiltered REE data from Lacan and Jeandel (2004b) from the NS. Waters with $\sigma_\theta < \sim 27.7$ show inverse gradients in the water column that slightly differ for each REE. Figure 5 shows REE concentrations normalized to Post-Archean Australian Sedimentary rocks (PAAS; McLennan, 2001) and to the sample BATS 15 m from the Bermuda Atlantic Time-Series (van de Flierdt et al., 2012), revealing typical patterns for open ocean seawater with a progressive enrichment from light REEs (LREEs) to heavy REEs (HREEs). The HREE to LREE ratios (here: $([Tm]_N+[Yb]_N+[Lu]_N)/([La]_N+[Pr]_N+[Nd]_N)$, whereby "N" refers to PAAS-normalized concentrations) are constant in waters with $\sigma_\theta > \sim 27.7$ (4.3, 1 SD = 0.3, n = 58), and overall lower in waters with $\sigma_\theta < \sim 27.7$ (3.8, 1 SD = 0.3, n = 44), with lowest ratios determined in NEGSSW (3.5, 1 SD 0.2, n = 13). A negative cerium anomaly is observed for all samples, and the Ce/Ce* ratio (defined as the $[Ce]_N/[([La]_N+[Pr]_N)/2]$) varies between ~0.10 (PW) and ~0.25 (mostly AW) at the surface with most samples having ~0.2. A slight decrease in Ce/Ce* from ~0.2 to ~0.1 is observed with depth.

The Nd isotopic compositions range between ε_{Nd} = -12.4 and -8.8 for all samples (Figs. 2-4 and 6). Waters with $\sigma_\theta > \sim 27.7$ and shallower than ~500 m (mostly classified as

15

AW/RAW) have relatively unradiogenic compositions (least radiogenic ε_{Nd} = -12.2±0.2) compared to intermediate and deep waters deeper than ~500 m depth (most radiogenic ε_{Nd} = -9.5±0.2), with the exception of station 68 that shows more radiogenic signatures in the upper ~500 m of the water column even if the potentially contaminated surface sample is not considered (Fig. 3). On the western Svalbard Shelf, a slightly more radiogenic Nd isotopic composition is also observed for surface waters (ε_{Nd} = -10.6±0.2). Waters with σ_θ < ~27.7 have different Nd isotopic compositions, largely following the distribution of the water masses defined by θ-S and nutrient properties. The NEGSSW has less radiogenic signatures (ε_{Nd} = -11.7, 1 SD = 0.5, n = 13), similar to AW/RAW samples. In contrast, PW and KW have more radiogenic εNd signatures including the most radiogenic sample of the data set (ε_{Nd} = -8.8±0.2). Such signatures are dominant in surface waters near ~5° W, but also can be found on the NE Greenland Shelf at ~150 m depth following the isoline of S ≈ 33 (Fig. 4). Deeper than this depth less radiogenic signatures with ε_{Nd} = -11.8 (1 SD = 0.2, n = 4) characterize NEGSBW.

At the Laptev Sea margin, water with typical θ-S characteristics of AAW has [Nd] = 16.4 pmol/kg and ε_{Nd} = -10.0±0.1 at ~200 m depth. Surface seawater (S ≈ 7) close to the Lena River delta has [Nd] = 556 pmol/kg and ε_{Nd} = -15.7±0.2.

5. DISCUSSION

5.1 Transport and modification of Nd isotopes in the Fram Strait

The waters occupying most of the Fram Strait water column (σ_θ > ~27.7) show no significant variations in dissolved [REE], in contrast to the dissolved Nd isotopic composition that changes from relatively unradiogenic values at shallow depths (< ~500 m) to more radiogenic values in intermediate and deep layers (Figs. 2, 3 and 6). The absence of vertical gradients in [Nd]$_{ID}$ (Fig. 3) and REE patterns (Fig. 5) between shallow, intermediate and deep waters and the differences in ε_{Nd} signatures between waters of the upper and the deeper water column

16

together clearly demonstrate that significant REE release from sinking organic or inorganic particles does not occur in the open Fram Strait, given that this would result in increasing [REE] and a change of the ε_{Nd} signatures of the intermediate and deep water masses towards the less radiogenic signatures of the upper waters. In contrast, the apparent oxygen utilization (AOU) increases with depth (contour lines in [Nd] plot of Fig. 3), which points to decomposition of organic matter that may result in REE release and a change of the ambient dissolved Nd isotope compositions. In the North Atlantic an increase in AOU is accompanied by either increasing [Nd] that is attributed to remineralization of organic particles below productive waters (Stichel et al., 2015) or constant [Nd] in regions of strong lateral advection (Lambelet et al., 2016). The latter scenario may be conceivable for the Fram Strait region, but almost constant [REE] are observed throughout the water column of the entire open AM (Andersson et al, 2008; Porcelli et al., 2009; Yang and Haley, 2016), indicating that remineralization of organic particles does not control the Nd isotope and REE distributions, not even in regions characterized by weak lateral advection (e.g. the deep central Canada Basin, Yang and Haley, 2016).

The most likely explanation for the absence of particulate REE release in the AM is the overall low primary productivity in the upper central AO due to the light limitation caused by a permanent sea-ice cover (Fernández-Méndez et al., 2015 and references therein), which results in low particle fluxes and in the suppression of significant vertical REE transport to intermediate and deeper layers. While the largest direct source of terrestrial REEs to the AM is the Arctic rivers (Fig. 1a), their impact on the vertical distribution of REEs in the open AM is limited, too. Recent experiments simulating Arctic estuarine mixing have shown that most of the particle-reactive riverine REEs are bound to inorganic nanoparticles and colloids that are removed from the water column through coagulation in the low-salinity range (Tepe & Bau, 2016). Most of the coagulated REE-bearing colloids are thus likely confined to the shelves, suggesting that potential remobilization of the REEs mainly occurs in proximity to

17

the coast. Their transport to the open AM is also inhibited by the Arctic Circumpolar Boundary Current (e.g. Aksenov et al., 2011) that transports AW and other waters along the Arctic margins (see also Fig. 1a) and thus prohibits direct advection of significant amounts of particles to the open AM. A limited amount of dissolved REEs is advected with the riverine freshwaters (Porcelli et al., 2009), which does, however, not affect the deeper waters below. Supported by the lack of significant vertical fluxes, the dissolved Nd isotope and REE distributions in the open AM mainly reflect lateral water mass advection and mixing, in agreement with recent findings by Yang and Haley (2016). Our data thus provides further evidence that the REEs exhibit conservative behavior in the entire open AM (in the NS at least down to ~2600 m depth) and that the dissolved Nd isotope distribution is dominantly controlled by lateral advection of water masses and their mixing.

In contrast, the Arctic shelf regions are clearly affected by particle-seawater interactions causing non-conservative REE and Nd isotope behavior (e.g. Dahlqvist et al., 2007; Porcelli et al., 2009). In the Fram Strait region, modification of [Nd] and the Nd isotope signature through remineralization of biogenic particles, remobilization of REEs from coagulated inorganic nanoparticles and colloids and/or REE release from detrital particles clearly occurs in bottom waters on the NE Greenland Shelf (i.e. NEGSBW). The NEGSBW was suggested to be ultimately of AW or RAW origin due to its relatively high temperatures (e.g. Budéus et al., 1997), the advection of AW or RAW on the NE Greenland Shelf from any direction, would however, also result in mixing with PW or KW and cause a shift in the Nd isotopic composition of AW (ε_{Nd} = -11.7, 1 SD = 0.4, n = 11, see section 5.2) towards more positive ε_{Nd} values. Yet, NEGSBW has ε_{Nd} values identical to AW (ε_{Nd} = -11.8, 1 SD = 0.2, n = 4) but significantly higher [Nd] (24.0 pmol/kg, 1 SD = 1.4) than that of AW (15.9 pmol/kg). These Nd characteristics neither reflect pure AW nor can they be explained through pure mixing between AW/RAW and PW or KW (see Fig. 8c and d). Positive AOU values (up to ~50 μmol/kg) and elevated Si concentrations ([Si] ≈ 8 μmol/kg, Fig. 6) instead point to

18

remineralization of biogenic particles formed in the unradiogenic NEGSSW to mostly account for the modification of the ε_{Nd} signatures towards less radiogenic values and higher [Nd] compared to the composition expected from mixing of AW with PW or KW. Remineralization processes have been previously suggested to be common for the area east of the Northwind Shoal (Budéus et al., 1997). The Nd isotopic composition of NE Greenland Shelf particles and surface sediments is unknown, but is likely similar to the highly unradiogenic composition of rocks from NE Greenland ($\varepsilon_{Nd} \approx$ -18, 1 SD = 9.5, n = 45, all samples including references are reported in the electronic supplement C). Relatively long residence times (10-20 years) of NEGSBW on the shelf are evident from transient tracer data obtained during the same cruise (Stöven et al., 2016) and are in agreement with previous studies (Budéus et al., 1997; Top et al., 1997) thus promoting seawater-particle interactions and remineralization processes.

5.2 Origin and fate of Atlantic Water

5.2.1 Composition and distribution of AW and RAW at Fram Strait

The unradiogenic ε_{Nd} values of the upper water column in the eastern and central Fram Strait clearly correlate with the distribution of warm and saline AW entering the AO via the WSC (Fig. 3). Representative AW samples (S > 35.0; θ > 3 °C; 27.70 < σ_θ ≤ 27.97) have an average ε_{Nd} of -11.7 (1 SD = 0.4, n = 11) and [Nd] = 15.9 pmol/kg (1 SD = 0.5), similar to an AW sample collected in 2011 at the same latitude (ε_{Nd} = -11.9±0.27 and [Nd] = 16.8 at 150 m depth; Werner et al., 2014) and three AW samples collected in 2001 in the upper water column north of Svalbard (average ε_{Nd} = -11.8 with 1 SD = 0.5 and [Nd] = 16.6 with 1 SD = 0.2; Andersson et al., 2008). These data are also identical to two unfiltered samples from the upper water column collected in 1999 at ~77.7° N and ~7.7° E (average ε_{Nd} of -11.5 with 1 SD = 0.4; data from station 29, Lacan, 2002). Our high resolution data also show that the least radiogenic ε_{Nd} signatures within the AW layer are observed at stations 19, 26 and 55 (Fig. 3)

19

and seperated through waters with slightly more radiogenic signatures and lower salinities at ~5° E. This distribution might either reflect the cores of the Yermak (at ~3.7° E) and Svalbard (at ~7° E) branches of the AW (e.g. Rudels et al., 2000; Walczowski et al., 2005), or document the eddy activity in the region (e.g. Hattermann et al., 2016; von Appen et al., 2016).

The identification of a distinct AW signature with an ε_{Nd} = -11.7 in the Fram Strait is not consistent with the previous assumption that all waters entering the AO have a homogeneous ε_{Nd} signature of -10.8 (cf. Andersson et al., 2008; Porcelli et al., 2009). This misconception was mainly a result of the lack of data with typical θ-S characteristics of AW (e.g. no Nd samples were collected in depths < ~600 m in the eastern Fram Strait before 2011). Instead, inputs from Svalbard shelf sediments were invoked to account for the less radiogenic compositions of samples collected in 2001 north of Svalbard (Andersson et al., 2008), which is in agreement with relatively high [Nd] (up to 30 pmol/kg) determined in samples shallower than ~100 m depth but not consistent with the low [Nd] of the three above-mentioned AW samples recovered below ~100 m in 2001. This suggests that either inputs from Svalbard shelf sediments increase [Nd] in waters without significantly affecting the Nd isotopic composition or that waters with relatively high [Nd] but similar ε_{Nd} signatures are admixed to the upper water column north of Svalbard. The samples with the relatively high [Nd] exhibit slightly lower salinities compared to the three AW samples, which is consistent with admixture of small quantities of freshwater and argues against lithogenic Nd input from Svalbard.

Our surface samples recovered on the Svalbard continental shelf in addition argue against any Nd input from western Svalbard to the Fram Strait region. The shift towards more radiogenic ε_{Nd} values (-10.6±0.19 in near surface sample next to the ship) and lower [Nd] (~15 pmol/kg) and S (~34.5) in comparison to AW points to contribution of surface waters with sea-ice meltwater, provided that less Nd is released from the sea ice during melting than

20

initially present in the water of the melting area (i.e. resulting in dilution of Nd). Input of Nd from Svalbard would likely result in an increase in [Nd] and yield a shift towards less radiogenic Nd isotopic compositions, as indicated by the relatively unradiogenic ε_{Nd} signatures of beach deposits of western Spitsbergen (Fig. 1b). The latter are relatively uniform with an average ε_{Nd} of -14.6 (1 SD = 1.84, n = 6) and perhaps more suitable to evaluate Nd input from Svalbard than the variable ε_{Nd} signatures of Svalbard rocks (the range in rock ε_{Nd} values for particular Svalbard areas is shown in Fig. 1b; rock and beach deposit samples including references are provided in electronic supplement C). The small mean annual discharge (~20 km^3 for entire Svalbard) also argues against significant contributions of freshwater and Nd from Svalbard (Beszczynska-Möller et al., 1997 and references therein). We therefore instead suggest that the Nd isotope characteristics observed on the western Svalbard Shelf reflect the advection of Arctic-derived cold and less saline Polar Water with relatively high sea-ice meltwater fractions. These waters most likely originated in the Barents Sea and have been transported northward within the Sørkapp Current, an extension of the East Spitsbergen Current (Walczowski, 2013 and references therein).

Three shallow and intermediate samples of station 86 have ε_{Nd} values identical to AW (-11.6, 1 SD = 0.1), but most likely correspond to RAW as they are clearly separated from AW by more radiogenic ε_{Nd} signatures at ~1° E (station 68) (Fig. 3). This distribution indicates admixture of more radiogenic intermediate waters to shallower depths, which is consistent with lowered S and T at ~0.5° E. Mesoscale eddies generated in the WSC (von Appen et al., 2016) have been shown to be involved in the westward and subsequent southward transport of the Yermak Branch, with the most intensive recirculation occurring between 78° N and 81° N (e.g. Hattermann et al., 2016; Walczowski, 2013). These eddies might induce upwelling and thus perhaps were responsible for the vertical mixing of the more radiogenic Nd isotope signatures observed at station 68 in 2012. About half of the northward transport returns back into the NS without significant changes in θ-S characteristics (de Steur

21

et al., 2014; Marnela et al., 2013). The ε_{Nd} data also argue for little transformation of the returning waters and confirm that RAW returns immediately north of the Strait without significantly mixing with other waters. The Nd isotopes further suggest that modified RAW extends as far as the Greenland continental margin at depths between ~200 and ~400 m (below PW and KW), consistent with relatively high T and S observed at these depths (Fig. 3).

5.2.2 Modification of AW within the AM

Our new data and the compilation and reassessment of literature seawater Nd data collected at different locations within the AM provide evidence that the Nd isotopic composition of AW gradually changes during transport across the AM from unradiogenic signatures ($\varepsilon_{Nd} \approx$ -13) at the Greenland-Scotland Ridge (GSR) towards more radiogenic signatures ($\varepsilon_{Nd} \approx$ -9) in the Canada Basin (Fig. 7). Changes in θ, S and potential density characteristics within the AW layer were previously assigned to heat loss due to ice melting and exchange with the atmosphere and/or mixing with colder waters from the Barents Sea, the Bering Strait and with river runoff, resulting in the formation of the Atlantic-derived halocline water and a cooler ($\theta \leq 2$ °C) AAW (e.g. Rudels et al., 2015). The continuous change in θ, S and potential density in Nd samples compiled from different years implies that they can be used to assess general trends in Nd isotope characteristics and the processes causing them. In contrast to elevated [Nd] in AW samples from the Denmark Strait and the eastern Norwegian Sea/Lofoten Basin (> 19 pmol/kg), the [Nd] of most AW samples from other locations is uniform at ~16 pmol/kg (except Canada Basin), including the AW at the Iceland-Scotland Ridge (i.e. the main inflow area of AW, [Nd] = 16.2 pmol/kg, 1 SD = 2.1, n = 7) (Fig. 7b). This implies that local modification of Nd characteristics in AW samples from the Denmark Strait and the eastern Norwegian Sea/Lofoten Basin must have occurred and we consequently exclude these from further discussion of water mass mixing.

22

A change in the Nd isotopic composition without significant changes in [Nd] can be attributed to either admixture of other water masses with similar [Nd] or by seawater-particle exchange (i.e. boundary exchange; Jeandel and Oelkers, 2015). Intermediate waters below the AW layer in the whole AM have more positive ε_{Nd} values but [Nd] overall identical to AW except in the Iceland and Norwegian Seas (Fig. 7b). Admixture of such waters could explain the change in ε_{Nd} as well as T, S and potential density (Fig. 7c) as far as the Laptev Sea continental slope (in particular in the Nordic Seas, where deep water convection involves conversion of inflowing warm AW to deep cold water). Further north and east, admixture of old and dense Kara Sea shelf waters may cause additional shifts towards radiogenic ε_{Nd} without significantly affecting [Nd]. These waters may have acquired the ε_{Nd} signature of Yenisei and/or Ob freshwater but at the same time have low [Nd], since most of the riverine Nd may have likely been removed through coagulation of REE-bearing nanoparticles and colloids from the water column in the Kara Sea. In the Canada Basin, deep-water ventilation with involvement of relatively radiogenic PACW evolving from the Chukchi Sea with [Nd] around 30 pmol/kg could result in further modification towards more radiogenic ε_{Nd}, but also result in a slight increase in [Nd] (Porcelli et al., 2009).

Clearly, most of the compositions observed in the AW layer of the AM can be explained by admixture of the above-mentioned waters, which overall agrees with previous observations based on θ, S and potential density characteristics (e.g. Rudels et al., 2015) and which suggests that consideration of significant seawater-particle exchange is not required. Admixture of significant amounts of relatively radiogenic PW or KW that leaves the AO through Fram Strait would result in a strong increase in [Nd] and a decrease in S and thus cannot account for the observed change (Fig. 7a and b). Significant admixture of NCW is also unlikely, as this water mass has a less radiogenic ε_{Nd} (-14.5) than AW.

After transport through the AO, AW ultimately leaves the AO via the EGC as cold, modified AAW (e.g. Rudels et al., 2005). Our Nd data does not provide evidence for a

23

distinct AAW layer in 2012, but instead points to a water body that exhibits θ-S and potential density characteristics of dense AAW (dAAW). This water mass is observed in the western Fram Strait between ~3 and 5° W and between ~400 and ~900 m depth characterized by a homogeneous ε_{Nd} value of -10.4 (1 SD = 0.2, n = 5) and [Nd] = 16.3 (1 SD = 1.1). Based on our comparison with other AW samples from the AO, most of the dAAW observed at Fram Strait must have recirculated within the Eurasian part of the AO (see Fig. 7). This is also in agreement with the relatively low ventilation ages of dAAW (~30 years) based on transient tracer data (Stöven et al., 2016), which suggests that these waters took the short loop within the AO (cf. Tanhua et al., 2009). The fate of dAAW in the NS is unknown although its flow within the EGC at intermediate depths and its similar Nd isotopic composition to the precursor of Denmark Strait Overflow Water (Lacan and Jeandel, 2004a; in the electronic supplement A referred to as AIW/GS) indicates that a part of it leaves the NS within the Denmark Strait Overflow Water. Indeed, about half of the overflow water supplied from the AM to North Atlantic Deep Water has passed the AO (Rudels, 2009), which argues for a significant contribution of dAAW to the overflow.

5.2.3 AW as precursor of intermediate and deep waters

The AW/RAW and dAAW are the main precursors of intermediate and deep waters within the AM. Their mixture with other intermediate waters is not only reflected in a change of the composition of the AW layer, but also reflected in the gradual ε_{Nd} change of intermediate and deep waters from radiogenic signatures in the Iceland and Norwegian Seas and the Lofoten Basin (~ -8.1 to ~ -10.1; Lacan and Jeandel, 2004b) towards less radiogenic signatures in the AO ($\varepsilon_{Nd} \approx$ -10.7; Andersson et al., 2008; Porcelli et al., 2009; Zimmermann et al., 2009). However, conversion of AW/RAW and dAAW to intermediate and deep waters cannot account for the observed radiogenic ε_{Nd} values of the latter, reaching -9.5 in the Fram Strait. The source of these signatures is likely located in the Iceland and Norwegian Seas where the

most radiogenic ε_{Nd} signatures within the entire AM were observed in previous studies (i.e. ~ -8.1). Neodymium release from or boundary exchange with the basaltic formations of Iceland and Central-East Greenland is the most likely explanation for the more radiogenic intermediate and deep-water signatures (e.g. Lacan and Jeandel, 2004a), in good agreement with the slightly elevated [Nd] in intermediate waters of these regions (Fig. 7b). Andersson et al. (2008) also suggested boundary exchange along the Canadian archipelago to account for relatively unradiogenic ε_{Nd} signatures (~ -9.8) of intermediate waters northwest of the Fram Strait, as the limited data available for the Arctic inflow area at the time indicated a homogeneous ε_{Nd} composition of ~ -10.8 throughout the water column. Our new data clearly document that ε_{Nd} values around ~ -10 are present in the eastern and western Fram Strait below ~500 m, thus there is no evidence for such a process. The small ε_{Nd} variations below ~500 m do not clearly reflect the water masses defined by their hydrographic properties, which suggests that the intermediate and deep water masses in the AM are well mixed in terms of their Nd distribution.

5.2.4 Origin of AW prior to its entrance into the AM

The relatively unradiogenic ε_{Nd} signature of AW at the GSR most likely originates from contributions of modified Gulf Stream water and Labrador Current water from the North Atlantic. Waters with characteristics similar to AW at the GSR have been recently reported in the region around the Grand Banks and have been attributed to mixing between the Gulf Stream and the Labrador Current (Lambelet et al., 2016). The relatively unradiogenic ε_{Nd} signature observed in Labrador Sea waters thus most likely not only affects the Nd isotope distribution in the subpolar gyre, but is also responsible for modification of shallower waters within the North Atlantic Current that ultimately enter the AM. This is also in agreement with previous studies based on θ-S properties that identified cooler and slightly fresher Modified North Atlantic Water (MNAW) at the GSR in addition to North Atlantic Water (Hansen and

25

Østerhus, 2000 and references therein). A high contribution of MNAW in AW is further supported by the REE distribution of AW in the Fram Strait, which is characterized by [MREE] and [HREE] and slightly enriched [LREE] (except Ce) similar to the NW Atlantic Ocean (BATS 15 m and BATS 2000 m; van de Flierdt et al., 2012) and indicates that admixture of Labrador Sea waters mainly results in an increase of [LREE] (Fig. 5b).

5.3 Distribution, composition and fate of Arctic-derived waters

Despite several attempts to decipher the different fractional components within the Arctic-derived waters (e.g. Dodd et al., 2012; Falck, 2001; Falck et al., 2005; Jones et al., 2008b; Rabe et al., 2013; Taylor et al., 2003), a clear picture of the distribution, composition and fate of these waters is still missing, particularly because observations of the above mentioned studies do not agree with earlier results suggesting the contribution of locally formed waters in the western Fram Strait (Bignami and Hopkins, 1997; Budéus and Schneider, 1995; Budéus et al., 1997). The Arctic-derived waters discussed here (i.e. PW and KW) were defined based on findings of Budéus et al. (1997) and Bignami and Hopkins (1997), who used recurring θ-S features and silicate concentrations ([Si]) to distinguish between locally formed and imported water masses. However, the [Si] can be affected through biological production and remineralization processes, which in 2012 most likely caused low to zero [Si] in NEGSSW (Fig. 4) and elevated [Si] ≈ 8 μmol/kg in NEGSBW (Figs. 4 and section 5.1), respectively. Hence, the [Si] distribution reliably traces PW and KW only in areas where direct advection from the AO is evident. The general current distribution in Fram Strait and over NE Greenland Shelf (e.g. Beszczynska-Möller et al., 2012; Bourke et al., 1987; Woodgate et al., 1999) suggests that PW and KW are directly advected above the Greenland continental slope where they significantly contribute to the formation of the core of the EGC. The elevated [Si] at ~5 °W thus clearly can be attributed to PW imported from the AO and the associated relatively radiogenic ε_{Nd} signatures (including the most radiogenic value of the Fram Strait

26

section with ε_{Nd} = -8.8±0.2, $PW_{\varepsilon Nd-max}$) and elevated $[Nd]_{ID}$ (Fig. 1b, 3 and 4) also must have been directly imported from the AO and likely represent undiluted compositions of PW and KW. The relatively radiogenic values follow salinities of ~33 and [Si] > ~8 μmol/kg on the NE Greenland Shelf, pointing to the presence of PW on the shelf down to ~150 m depth and confirming that [Si] on the shelf can either be formed through local remineralization or can be imported from the AO (Budéus et al., 1997).

Neodymium isotope based mixing calculations show that most PW and KW samples lie close to the mixing line between AW that enters the AO through Fram Strait and modified Pacific Water leaving the Chukchi Sea shelf (PACW) (Fig. 8a and b). All PW and KW samples have too high [Nd] and too low S for their ε_{Nd} to directly plot on the mixing line and thus require contributions from a third end-member or a process to explain this offset. Arctic rivers constitute the second largest REE source in the AM (Fig. 1a and electronic supplement A) and dominate the Nd in the shallow waters (e.g. Porcelli et al., 2009). Their contribution is thus most likely responsible for the offset from the mixing line towards higher [Nd] and lower S (see also Andersson et al., 2008), which inhibits a quantitative assessment of the three end-members based on Nd isotopes alone since contributions of riverine Nd may originate from any of the major Arctic rivers and would result in differing increases in [Nd] and changes in ε_{Nd}. The mass balance calculations based on $\delta^{18}O$, S and nutrients (N/P and PO* methods) however provide further information on the composition and provide quantitative fractions for meteoric water. The amount of f_{MW} for the $PW_{\varepsilon Nd-max}$ sample that represents pure PW is ~6 to ~8 %, and for KW samples is even lower (< ~5 %), which documents a small amount of river water being present in the Arctic-derived waters in the Fram Strait. Although the initial [Nd] in rivers can be 100 times as high as in seawater most of the riverine Nd is removed in estuaries and on the Siberian shelves (Porcelli et al., 2009), which together with the low f_{MW} implies a relatively low contribution of riverine Nd to these waters and suggests that the shift of the ε_{Nd} signature caused by addition of riverine Nd was overall small. The ratio between

27

PACW and AW of $PW_{\epsilon Nd-max}$ thus likely is close to ~ 2:3, and results in Nd-based PACW fractions (f_{PACW}) as high as ~30 % for Arctic-derived waters (Fig. 8a and b). This Nd-based maximum f_{PACW} matches the maximum f_{PAC} (up to ~30 %) determined with the PO* method, but does not agree with the maximum f_{PAC} (up to ~70%) determined with the N/P method (see Fig. 4), pointing to uncertainties in end-member definitions for the calculation of the PAC fractions. In particular denitrification on the Siberian Shelves can result in overestimation of the N/P-based f_{PAC} (Anderson et al., 2013; Bauch et al., 2011), suggesting that the "Pacific-derived Water" end-member used in the N/P method does not represent a pure water mass composition. Despite these uncertainties, the contribution of PACW/PAC is supported by low Ce to Ce* ratios ("Ce anomaly") seen in PW samples that overall have the strongest Ce anomalies in surface waters of the entire Fram Strait section. A strong Ce anomaly can be attributed to continuous removal of $Ce(IV)O_2$ and may be indicative of the time a water mass was isolated from fresh, unfractionated continental inputs (Hathorne et al., 2015), which is in agreement with the age and the flow path of Pacific-derived water that must have traveled across the entire AO.

The origin of PW can be attributed to the Pacific-derived upper halocline (Jones and Anderson, 1986) and more shallow waters of the Canada Basin for S < 33 based on its [Si] and the salinity properties. Comparison with literature Nd data in addition suggests that PW is advected through the Amundsen and Makarov Basins (Fig. 8a and b), indicating transport of the Pacific-derived component of PW along the continental slope of the East Siberian Sea into the Transpolar Drift and the western Fram Strait (cf. Aksenov et al., 2016). An Atlantic origin was suggested for KW by previous studies due to the distinct θ-S properties and low [Si] (e.g. Budéus et al., 1997), as well as f_{PAC} close to 0 % (Falck, 2001). Rudels et al. (2005) have shown that waters with such θ-S properties form north of Svalbard, where melting of sea ice above the AW creates a less saline upper layer. Although f_{SIM} of our KW samples is negative or close to zero and therefore rather indicates addition of brine waters instead of sea-ice melt,

28

this does not contradict the formation process mentioned above given that freezing and melting may occur simultaneously during this process (Rudels et al., 1999a) and will result in different f_{SIM}. Furthermore, addition of SIM would most likely cause a decrease in Nd concentration (i.e. through dilution) without significantly affecting the Nd isotopic composition, the PACW to AW ratio thus would mostly remain unaffected. According to our Nd isotope mixing calculations the PACW to AW ratio of KW is about 1:4, which confirms a high contribution of AW (~80 %) (Fig. 8a and b). The comparison with literature Nd data from the AM shows that KW shares characteristics with shallow samples from the Nansen Basin (Fig. 8a and b), and thus further supports the origin of these waters to be located north of Svalbard.

South of Fram Strait both PW and KW can be traced along the Greenland continental slope as far as the Denmark Strait. While shallow waters of the southern and western NS only show minor amounts of these waters, most of the Nd isotope characteristics of shallow waters of the EGC at 73 and 77° N and the Denmark Strait can be explained by their advection and admixture of AW from the ISR, the Denmark Strait or the Fram Strait (Fig. 8c and d). An increase in [Nd] and S in PW samples that have less radiogenic ε_{Nd} values compared to $PW_{\varepsilon Nd-max}$ (resulting in modified PW, PW_{mod}) indicates local admixture of NEGSBW (Fig. 8c and d) after its interaction with Greenland shelf sediments (section 5.1), which results in an increase in [Nd] and a shift towards lower ε_{Nd} at constant S. In contrast, addition of Greenland freshwater (GFW) causes an increase in [Nd] and a decrease in salinity, while the ε_{Nd} signature is shifted towards less radiogenic values (section 5.4). Both processes could also account for the composition of samples obtained from the Denmark Strait, while samples from the EGC at 73 and 77° N do not show such a pronounced interaction with GFW or NEGSBW.

We point out that the composition of PW and KW presented in this study represents only a snapshot of the water mass distribution in the Fram Strait (i.e. summer 2012). Several

studies have shown that the f_{MW}, f_{SIM} and f_{PAC} of PSW that leaves the AO through the western Fram Strait exhibit seasonal as well as interannual variability (e.g. Dodd et al., 2012; Falck, 2001; Falck et al., 2005; Jones et al., 2008b; Rabe et al., 2013; Taylor et al., 2003). Future multi-year surveys that include Nd isotope and REE measurements will test the promising sensitivity of Nd isotopes and REEs to reflect and quantify these changes.

5.4 Admixture of Greenland freshwater

Studies carried out in the mid-1990s pointed to contribution of locally formed waters on the NE Greenland Shelf (Bignami and Hopkins, 1997; Budéus and Schneider, 1995; Budéus et al., 1997). Bignami and Hopkins (1997) in particular suggested that shelf surface waters that show a "fanning out" of the temperature below S ~32 in the θ-S field can be attributed to local runoff and modification by local heating and ice melting, while shelf intermediate waters (S ~32) form convectively through loss of buoyancy to the atmosphere with the surface waters as the source waters. These findings are supported by a substantial change from ε_{Nd} = -8.8 ($PW_{\varepsilon Nd\text{-}max}$) to ε_{Nd} ≈ -12 (NEGSSW) observed on the shelf of Greenland, which is accompanied by an increase in [Nd] and a slight decrease in HREE/LREE and S (Figs. 4 and 8). A concurrent increase in f_{MW} from ~6-8 % to ~13 % at first glance would in combination with the shift in ε_{Nd} suggest additional contribution from an Arctic river with relatively unradiogenic Nd isotopic composition (e.g. Mackenzie or Lena River, Fig. 1a). Surface samples obtained from the Amundsen and Makarov Basins with likely high fractions of riverine Nd indeed document characteristics similar to NEGSSW and may thus be the origin of NE Greenland Shelf waters. However, it is unlikely that the relatively unradiogenic ε_{Nd} signatures observed in shallow waters of the central AO would be preserved during their transport to the NE Greenland Shelf, as admixture of PW and KW would modify these signatures towards more positive ε_{Nd} values. We therefore suggest that the source of the Nd and the isotopic composition of NEGSSW is local and located west of the EGC.

The freshwater flux from Greenland to the AM was ~200 km^3/yr in 2010, with a general trend towards increasing fluxes in the last few decades (Bamber et al., 2012). Contribution of GFW (precipitation and Greenland Ice Sheet melt) to coastal and shelf waters off Greenland was recently investigated by Stedmon et al. (2015). Their data from the same year as our cruise (September) and the same location indicate GFW fractions (f_{GFW}) as high as ~4 % for waters with θ-S properties similar to NEGSSW, which clearly points to significant changes of the Nd characteristics, in agreement with the shift observed between PW/KW and NEGSSW. Dissolved [REE] in glacial-derived waters from western Greenland for example are ~60 times higher (for [Nd]) than those of typical seawater and indicate significant input of REEs from Greenland to the North Atlantic (Tepe and Bau, 2015). Similarly, high [Nd] (~100 pmol/kg) and $\varepsilon_{Nd} \approx$ -3.5 have been reported for East Greenland Shelf waters (30.5 < S < ~33) at 68° N and were suggested to derive from lithogenic inputs from Greenland (Lacan and Jeandel, 2004a).

For our study area, we assume that all river water (this is f_{MW} if precipitation is neglected) contained within PW is derived from the AO and that the difference between f_{MW} of PW and NEGSSW was caused by GFW addition. The resulting δ^{18}O and salinity based mixing calculation shows that f_{GFW} reaches ~6 % in NEGSSW (Fig. 9a), which is similar to estimates of Stedmon et al. (2015) based on calculations involving δ^{18}O and colored dissolved organic matter. The presence of brines ($f_{SIM} < 0$) and sea-ice melt ($f_{SIM} > 0$) results in small offsets from our mixing line. The Nd isotopic composition of the GFW end-member is unknown, but is assumed to be relatively unradiogenic based on Nd isotopic compositions of rocks from NE Greenland (samples including references are reported in the electronic supplement C). We used the average rock Nd isotopic composition ($\varepsilon_{Nd} \approx$ -18, 1 SD = 9.5, n = 45) and adjusted the Nd concentration of the GFW end-member until the mixing line matched the f_{GFW} of the surface sample with the highest [Nd], resulting in [Nd] = 210 pmol/kg, which is within the range of concentrations reported for glacier-derived waters from other sites (e.g.

31

Lacan and Jeandel, 2004a; Tepe and Bau, 2015) and supports our hypothesis that the admixture of GFW is the cause of changes in Nd isotopes and REEs. Note, however, that the calculation of [Nd] does not account for any REE removal during salt-induced coagulation of REE-bearing nanoparticles and colloids in the low-salinity range (e.g. Tepe and Bau, 2016), which contrasts with REE release assumed to be significant only in NEGSBW, i.e. after the aggregated nanoparticles and colloids reached the depth of remineralization (~200 m, see section 5.1).

Strikingly, as seen in Fig. 9b, the expanded Nd isotope mixing calculation also reveals that the sea-ice related changes observed for $\delta^{18}O$ and salinity likely are also mirrored by the [Nd], resulting in too low [Nd] in NEGSSW surface samples (~10 m depth) and too high [Nd] in NEGSSW intermediate depth samples (~60 m) for their f_{GFW}. This supports that sea-ice melting may account for the decrease in [Nd] (i.e. through dilution), while sea-ice formation results in a brine signal that may account for excess [Nd]. The ε_{Nd} signature changes towards higher values for all samples (Fig. 9c), suggesting either that the Nd isotopic composition changes during addition of both brine and sea-ice meltwater, or indicating that the GFW end-member Nd isotopic composition is slightly more radiogenic than we assumed (e.g. $\varepsilon_{Nd} = -14$, Fig. 9c). Nevertheless, all REEs of NEGSSW samples are enriched in comparison to PW and resemble REE characteristics of glacially fed rivers from western Greenland characterized by relative enrichments of LREEs compared to HREEs (Tepe and Bau, 2015), further supporting GFW addition.

The distribution of GFW on the NE Greenland Shelf and the near-surface anticyclonic circulation scheme (e.g. Budéus et al., 1997; Rabe et al., 2009) both argue for a local source of GFW (e.g. the NE Greenland Ice Stream and its ice tongues Nioghalvfjerdsbræ/79° N Glacier and the Zachariæ Isstrøm) and provide further evidence for the GFW distribution to be restricted to the Greenland Shelf area (e.g. Hopwood et al., 2015). The strong EGC most likely also plays a major role for the entrapment of GFW on the Greenland Shelf. Future

32

potential changes of its strength and eddy variability might regulate the advection of GFW to the central NS and therefore to sites of open-ocean deep convection.

6. SUMMARY AND CONCLUSION

This work presents seawater Nd isotope (ε_{Nd}), rare earth element (REE) and stable oxygen isotope ($\delta^{18}O$) data from the Fram Strait and the NE Greenland Shelf obtained on samples collected during the ARKXXVII/1 expedition (June-July 2012). A comparison with hydrographic parameters, biogeochemical data and fractions of different water masses calculated with $\delta^{18}O$, salinity and nutrient based methods allows a comprehensive evaluation of prevailing water masses with implications for the understanding of the circulation within the Arctic Mediterranean (AM).

- Neodymium isotope and REE distributions in the open Fram Strait primarily reflect lateral advection of water masses and their mixing, while any significant influence of vertical processes is not observed. This is likely valid for the entire open AM (in the Nordic Seas at least down to 2600 m) and has implications for paleoceanographic reconstructions.

- Remineralization of biogenic and/or release from detrital particles is recorded in bottom waters on the NE Greenland Shelf and results in a shift towards less radiogenic ε_{Nd} signatures and elevated silicate concentrations. Silicate is either released locally or advected from the Arctic Ocean (AO).

- Atlantic Water (AW) enters the AO through the eastern Fram Strait and is characterized by $\varepsilon_{Nd} = -11.7$ and [Nd] $\approx$ 16 pmol/kg. This Nd isotope composition of AW is less radiogenic than previously reported and should be used for future oceanographic and paleoceanographic studies. The admixture of intermediate waters, dense Kara Sea waters and Pacific-derived waters to AW within the AM is

33

documented by a continuous change towards more radiogenic ε_{Nd} signatures and decreasing temperatures and salinities. Based on these changes, we confirm that Recirculating Atlantic Water and dense Arctic Atlantic Water (dAAW) return to the Nordic Seas (NS) within the Fram Strait and the Eurasian Basin of the AO, respectively. These waters then significantly contribute to the East Greenland Current (EGC) and part of the dAAW leaves the NS within the Denmark Strait Overflow Water. Significant inputs of Nd from Svalbard to the AW layer are not observed and surface waters on the Svalbard shelf are attributed to Polar Water from the Barents Sea with minor contributions of sea-ice meltwater.

- Intermediate and deep waters have relatively radiogenic ε_{Nd} signatures (reaching -9.5) that were acquired in the SW Nordic Seas (i.e. close to sites of deep water convection) and likely result from Nd inputs from basaltic formations of Iceland and Central-East Greenland. In terms of their Nd distribution, the intermediate and deep-water masses in the AM are well mixed.

- Arctic-derived shallow waters (Polar Water, PW and Knee Water, KW) are found in the western Fram Strait and are characterized by relatively radiogenic ε_{Nd} signatures (reaching -8.8) and variable [Nd] (21 to 29 pmol/kg). Both Nd characteristics and assessments based on S, ^{18}O and nutrients suggest that PW and KW were mostly composed of different proportions of Pacific- (< ~30 %, based on Nd isotopes) and Atlantic-derived waters, as well as of river waters (< ~8 %) in 2012. The fraction of Pacific-derived waters estimated by our approach based on Nd isotopes is in line with that computed with the PO* method, but differs significantly from that computed with the N/P method likely due to end-member uncertainties of the latter. While the PW composition resembles that of the Pacific-derived upper halocline and is most likely advected through the Amundsen and Makarov Basins, higher fractions of AW are evident in the KW, which shares characteristics of previously published Nd data from

34

the Nansen Basin and most likely formed through mixing between AW and sea-ice meltwater. After PW and KW pass the Fram Strait and enter the NS, they mix with AW and constitute a significant fraction of shallow waters of the EGC.

- The admixture of locally discharged Greenland freshwater (GFW) to PW is traced by Nd characteristics and an elevated meteoric water fraction and results in newly formed NE Greenland Shelf Shallow Water (NEGSSW). The amount of GFW in NEGSSW is estimated to be ~6 %. Due to the near-surface anticyclonic circulation on the shelf, this water mass is distributed and accumulated above the shelf and most likely does not enter the central NS directly, which may change in the future due to increasing meltwater inputs and may then have implications for deep convection in the NS.

- The pronounced gradients in ε_{Nd} signatures and REE characteristics in the upper water column of the AM together with $\delta^{18}O$ and standard hydrographic tracers provide a new basis to determine shallow hydrological changes within the AM.

35

FIGURE AND TABLE CAPTIONS

Table 1.

Summary of salinity and Nd characteristics of REE sources in the AM and water masses observed in Fram Strait in 2012. All samples used to determine the compositions of REE sources are listed in the electronic supplement A.

Figure 1.

Bathymetric map of the AM with an inset representing the Fram Strait region (IBCAO; Jakobsson et al., 2012). **a)** Map of the AM with circulation scheme of the upper layers (dashed white and grey lines) and the subsurface Atlantic and intermediate layers (solid black lines) (modified after Rudels et al., 2012). Circled crosses indicate sites of convection or sinking from intermediate and AW layers to deeper levels. The ε_{Nd} distribution is color-coded and shown for REE sources (colored rounded boxes with εNd values) and shallow seawater samples compiled from literature (colored circles) (Andersson et al., 2008; Lacan and Jeandel, 2004a, b; Piepgras and Wasserburg, 1987; Porcelli et al., 2009; Werner et al., 2014; Zimmermann et al., 2009). Only seawater samples from depths shallower than 60 m and uncertainties (2σ) better than 0.7 are shown. Rare earth element sources with known εNd values and [Nd] are Atlantic Water (AW) entering through the Iceland-Scotland Ridge (AW-ISR) and the Denmark Strait (AW-DS) (Lacan and Jeandel, 2004a, b), Norwegian Coastal Water (NCW; Petrova, 2015), Pacific-derived water (PACW; Dahlqvist et al., 2007; Porcelli et al., 2009) and major Arctic rivers (Persson et al., 2011; Porcelli et al., 2009; Zimmermann et al., 2009). Bold black arrows indicate mean freshwater flux from Greenland into the Arctic Ocean and the Nordic Seas for the year 2010 (Bamber et al., 2012). The estimated Nd inputs of the corresponding sources are given as percentage of the total Nd input into the AM taking into account volume transport and [Nd] of the sources (only rivers with discharges > 100

km^3/yr are considered). Further information on the REE sources of the AM is provided in the electronic supplement A.

b) Fram Strait region with the four major currents (WSC, West Spitsbergen Current; EGC: East Greenland Current; NEGCC: North-East Greenland Coastal Current; SC, Sørkapp Current) and ε_{Nd} data from literature (seawater: circles; rocks: black rounded boxes, supplement C) and this study (colored diamonds). The near-surface baroclinic circulation on the NE Greenland Shelf (bathymetry nomenclature after Arndt et al., 2015) is shown as black arrows with the length of the arrows indicating flow speed (Bourke et al., 1987). A clear distinction in the Nd isotopic signature is seen between AW (mean ε_{Nd} = -11.7, 1SD = 0.4, n = 11), Arctic-derived waters (Polar Water, PW and Knee Water, KW; most radiogenic ε_{Nd} = -8.8) and locally formed NE Greenland Shelf Shallow Water (NEGSSW; mean εNd = -11.7, 1 SD = 0.5, n = 13). More radiogenic ε_{Nd} signatures on the western shelf of Svalbard document Arctic-derived cold and less saline waters transported northward with the SC, which is an extension of the East Spitsbergen Current (Walczowski, 2013 and references therein). White arrows indicate marine outlets of the NE Greenland Ice Stream with Nioghalvfjerdsbræ (79° N Glacier; north arrow) and Zachariæ Isstrøm (south arrow) indicating the major source areas of Greenland freshwater (GFW) on the NE Greenland Shelf.

Figures were produced using Ocean Data View (Schlitzer, 2016) and modified manually. For interpretation of colors in this figure, the reader is referred to the web version of this article.

Figure 2.

Potential temperature (°C) versus salinity plots with potential density isopycnals (solid back lines; σ_θ, $\sigma_{0.5}$ and $\sigma_{1.5}$ = potential density at reference pressures 0 m, 500 m and 1500 m, respectively), together with εNd values (main plot, insets A and B) and [Si] (inset in main plot representing identical S and θ ranges) shown as color-coded circles. Additionally shown are

all CTD data from the cruise with highlighted selected stations (26, 55, 86, 106 and 126). Waters with $\sigma_\theta > \sim 27.7$ are classified based on the basis of constant θ-S end-member definitions (after Rudels et al., 2012; 2005) and for waters with $\sigma_\theta < \sim 27.7$ (confined to the NE Greenland Shelf and the upper water column above the Greenland continental margin), we applied a classification based on findings of Bignami and Hopkins (1997) and Budéus et al. (1997). Water masses are labeled as follows: Polar Water – PW, Knee Water - KW, NE Greenland Shelf Shallow Water – NEGSSW, NE Greenland Shelf Bottom Water – NEGSBW, Atlantic Water – AW, Recirculating Atlantic Water – RAW, Arctic Atlantic Water – AAW, dense Arctic Atlantic Water – dAAW, Upper Polar Deep Water – UPDW, Arctic Intermediate Water – AIW and deep waters – DW. DW is further subdivided in inset B to Nordic Seas Deep Water – NDW, Canada Basin Deep Water – CBDW, Eurasian Basin Deep Water – EBDW and Greenland Sea Deep Water – GSDW. (/) indicates unstable stratification in salinity or temperature, (\) indicates stable stratification in both salinity and temperature (Rudels et al., 2005).

Plots produced using Ocean Data View (Schlitzer, 2016) and modified manually. For interpretation of colors in this figure, the reader is referred to the web version of this article.

Figure 3.

Distribution of the salinity (all CTD data), the Nd isotopic composition (ε_{Nd}) and the Nd concentration measured with the isotope dilution method ($[Nd]_{ID}$, in pmol/kg) along the latitudinal section at 78.8° N. On the salinity and ε_{Nd} sections, distinct potential density (black, red and green solid lines) and potential temperature (0 °C, white dashed lines) isopycnals are also shown (see Rudels et al., 2012; 2005). On the salinity plot S = 34.915 is also shown as thin black contour lines. Similarly, for $[Nd]_{ID}$, the apparent oxygen utilization (AOU, in µmol/kg) is shown as thin black contour lines. The distribution of water masses as defined in the text and in Fig. 2 is indicated in the salinity plot. The numbers of the stations

38

where Nd isotope samples were taken are given above the ε_{Nd} plot. Similarly, the locations of stations with salinity profiles are shown as inverted triangles above the salinity plot. The selected stations shown in Fig. 2 are highlighted with the same color.

Sections produced using Ocean Data View (Schlitzer, 2016) and modified manually. For interpretation of colors in this figure, the reader is referred to the web version of this article.

Figure 4.

Distribution of distinct measured and calculated parameters of the uppermost 400 m on the NE Greenland Shelf and above the Greenland margin. Fractions computed with the N/P and PO* methods (Bauch et al., 2011) are: Meteoric water – $f_{MW-N/P}$, sea-ice meltwater – $f_{SIM-N/P}$, Pacific-derived Water – $f_{PAC-N/P}$ and $f_{PAC-PO*}$. Water masses as defined in the text and in Fig. 2 are schematically indicated on the ε_{Nd} plot. Here, distinction between PW samples modified through admixture of NEGSBW (PW_{mod}) and the most radiogenic PW sample ($PW_{\varepsilon Nd-max}$) is made. Contour lines of salinity (32, 33 & 34) and potential temperature (0 °C) are shown as black dashed and white lines, respectively. Names of stations with Nd samples are given above the ε_{Nd} plot (selected stations shown in Fig. 2 are highlighted with the same color) and for stations with nutrient and $\delta^{18}O$ samples above [Si].

Sections produced using Ocean Data View (Schlitzer, 2016) and modified manually. For interpretation of colors in this figure, the reader is referred to the web version of this article.

Figure 5.

a) Post-Archean Australian Shale (PAAS; McLennan, 2001) normalized REEs (plotted on log scale). Averages of selected water masses (as introduced in Fig. 2 and IWall = all

39

intermediate waters, DWall = all deep waters) are plotted together with Bermuda surface water (BATS15) and Bermuda deep water (BATS 2000) (van de Flierdt et al., 2012).

b) Bermuda surface water (BATS15) normalized REEs.

For interpretation of colors in this figure, the reader is referred to the web version of this article.

Figure 6.

Salinity versus ε_{Nd}, $[Nd]_{ID}$ and HREE/LREE (PAAS-normalized), as well as interpolated silicate concentrations ($[Si]_{interp}$, in µmol/kg) versus εNd plots for all samples (grey dots) and distinct water masses (see legend) as defined in text. The composition of NEGSBW does not correspond to what can be expected from mixing between AW/RAW and PW or KW, but rather suggests that local remineralization occurred and resulted in an increase of [Si] and a shift towards less radiogenic ε_{Nd} signatures (orange arrow).

Plots produced using Ocean Data View (Schlitzer, 2016) and modified manually. For interpretation of colors in this figure, the reader is referred to the web version of this article.

Figure 7.

Assessment of the composition of AW within the AM. Only samples with θ > 0 °C (all) and $27.70 < \sigma_{\theta} \le 27.97$ (AW & AAW within the Arctic Ocean) have been used. Atlantic-derived water entering the AM through the Iceland-Scotland Ridge is modified subsequently towards more radiogenic compositions through admixture of intermediate waters, dense Kara Sea waters and Pacific-derived waters. Admixture of Norwegian Coastal Water (NCW) or Polar Water (PW) cannot account for the observed compositions of AW samples. Light and dark green areas are the compositional fields of intermediate waters from the entire AM and the Iceland and Norwegian Seas, respectively.

40

For interpretation of colors in this figure, the reader is referred to the web version of this article.

Figure 8.

a) and b) Assessment of the Arctic source of PW and KW. The most radiogenic PW sample (PW$_{\epsilon Nd-max}$) can be explained by admixture of mainly AW and PACW and a small amount (6-8 %) of river water (red arrows). The AW to PACW ratio for PW$_{\epsilon Nd-max}$ is about 3:2, while it is for KW 4:1, with less amount of river water (< 5 %). PW$_{\epsilon Nd-max}$ shares characteristics with shallow samples ($\sigma_\theta \leq 27.7$, $\theta \leq 0$ °C) from the Amundsen and Makarov Basins, while characteristics of KW more closely match those of shallow samples from the Nansen Basin.

c) and d) Assessment of the fate of PW and KW in the Nordic Seas. Shallow waters in the Nordic Seas ($\sigma_\theta \leq 27.7$) can be mostly explained as a mixture of Polar Water exiting the AO through the western Fram Strait (here represented as PW$_{\epsilon Nd-max}$ and KW) and Atlantic-derived water from the Iceland-Scotland Ridge (AW-ISR), the Denmark Strait or the Fram Strait. Modified PW samples (PW$_{mod}$) show an increase in [Nd] and S, which can be attributed to admixture of NEGSBW (pink arrows). Modification through Greenland shelf sediments is observed in NEGSBW towards higher [Nd] and less radiogenic ϵ_{Nd} signatures at constant salinities (orange arrows). In contrast, addition of Greenland freshwater (GFW) is documented in NEGSSW with a strong increase in [Nd] and a decrease in salinities (blue arrows). Most of the samples within the EGC and the Denmark Strait show either modification through Greenland shelf sediments or addition of GFW. Samples from the southern and western Nordic Seas do not show significant contribution of Arctic-derived PW and KW.

For interpretation of colors in this figure, the reader is referred to the web version of this article.

Figure 9.

Mixing between Greenland freshwater (GFW; $\delta^{18}O$ = -23.4 ‰; ε_{Nd} = -18; [Nd] = 210 pmol/kg; S = 0; f_{MW} = 100%) and Polar Water (PW *average*; $\delta^{18}O$ = -1.5 ‰; ε_{Nd} = -9.9; [Nd] = 27.1 pmol/kg; S ~33; f_{MW} = 0%) on the NE Greenland Shelf. a) $\delta^{18}O$ against salinity, b) and c) [Nd]$_{ID}$ and ε_{Nd} against GFW in percent, respectively. The composition of NEGSSW can be explained by up to ~6 % addition of GFW, but offsets from the mixing line indicate that sea-ice melting and brine formation also affect $\delta^{18}O$ and salinity, as well as [Nd] and Nd isotopes. An alternative mixing line (grey) is shown in c) representing admixture of GFW with a more radiogenic ε_{Nd} signature (ε_{Nd} = -14).

For interpretation of colors in this figure, the reader is referred to the web version of this article.

REFERENCES

Aagaard, K., Foldvik, A. and Hillman, S.R. (1987) The West Spitsbergen Current - Disposition and Water Mass Transformation. *J Geophys Res-Oceans* **92**, 3778-3784. http://dx.doi.org/10.1029/JC092iC04p03778

Aagaard, K., Swift, J.H. and Carmack, E.C. (1985) Thermohaline Circulation in the Arctic Mediterranean Seas. *J Geophys Res-Oceans* **90**, 4833-4846. http://dx.doi.org/10.1029/JC090iC03p04833

Aksenov, Y., Ivanov, V.V., Nurser, A.J.G., Bacon, S., Polyakov, I.V., Coward, A.C., Naveira-Garabato, A.C. and Beszczynska-Moeller, A. (2011) The Arctic Circumpolar Boundary Current. *Journal of Geophysical Research* **116**. http://dx.doi.org/10.1029/2010jc006637

Aksenov, Y., Karcher, M., Proshutinsky, A., Gerdes, R., de Cuevas, B., Golubeva, E., Kauker, F., Nguyen, A.T., Platov, G.A., Wadley, M., Watanabe, E., Coward, A.C. and Nurser, A.J.G. (2016) Arctic pathways of Pacific Water: Arctic Ocean Model Intercomparison experiments. *J Geophys Res-Oceans* **121**, 27-59. http://dx.doi.org/10.1002/2015jc011299

Alkire, M.B., Morison, J. and Andersen, R. (2015) Variability in the meteoric water, sea-ice melt, and Pacific water contributions to the central Arctic Ocean, 2000-2014. *J Geophys Res-Oceans* **120**, 1573-1598. http://dx.doi.org/10.1002/2014jc010023

Anderson, L.G., Andersson, P.S., Bjork, G., Jones, E.P., Jutterstrom, S. and Wahlstrom, I. (2013) Source and formation of the upper halocline of the Arctic Ocean. *J Geophys Res-Oceans* **118**, 410-421. http://dx.doi.org/10.1029/2012jc008291

Andersson, P.S., Porcelli, D., Frank, M., Bjork, G., Dahlqvist, R. and Gustafsson, O. (2008) Neodymium isotopes in seawater from the Barents Sea and Fram Strait Arctic-Atlantic gateways. *Geochimica Et Cosmochimica Acta* **72**, 2854-2867. http://dx.doi.org/10.1016/j.gca.2008.04.008

Anisimov, O.A., Vaughan, D.G., Callaghan, T.V., Furgal, C., Marchant, H., Prowse, T.D., Vilhjálmsson, H. and Wals, J.E. (2007) Polar regions (Arctic and Antarctic). *Climate Change 2007: Impacts, Adaptation and Vulnerability. Contribution of Working Group II to the Fourth Assessment Report of the Intergovernmental Panel on Climate*

Change (eds Parry, M. L., Canziani, O. F., Palutikof, J. P., van der Linden, P. J., Hanson, C.E.) **15**, 653-685.

Arndt, J.E., Jokat, W., Dorschel, B., Myklebust, R., Dowdeswell, J.A. and Evans, J. (2015) A new bathymetry of the Northeast Greenland continental shelf: Constraints on glacial and other processes. *Geochemistry, Geophysics, Geosystems* **16**, 3733-3753. http://dx.doi.org/10.1002/2015gc005931

Arsouze, T., Dutay, J.C., Lacan, F. and Jeandel, C. (2009) Reconstructing the Nd oceanic cycle using a coupled dynamical – biogeochemical model. *Biogeosciences* **6**, 2829-2846. http://dx.doi.org/10.5194/bg-6-2829-2009

Bamber, J., van den Broeke, M., Ettema, J., Lenaerts, J. and Rignot, E. (2012) Recent large increases in freshwater fluxes from Greenland into the North Atlantic. *Geophysical Research Letters* **39**. http://dx.doi.org/10.1029/2012gl052552

Bauch, D., van der Loeff, M.R., Andersen, N., Torres-Valdes, S., Bakker, K. and Abrahamsen, E.P. (2011) Origin of freshwater and polynya water in the Arctic Ocean halocline in summer 2007. *Progress in Oceanography* **91**, 482-495. http://dx.doi.org/10.1016/j.pocean.2011.07.017

Beszczynska-Möller, A. (2013) The expedition of the research vessel "Polarstern" to the Arctic in 2012 (ARK-XXVII/1). *Berichte zur Polar-und Meeresforschung = Reports on polar and marine research* **660**. http://dx.doi.org/10013/epic.41150.d007

Beszczynska-Möller, A., Fahrbach, E., Schauer, U. and Hansen, E. (2012) Variability in Atlantic water temperature and transport at the entrance to the Arctic Ocean, 1997-2010. *ICES Journal of Marine Science* **69**, 852-863. http://dx.doi.org/10.1093/icesjms/fss056

Beszczynska-Möller, A., Weslawski, J.M., Walczowski, W. and Zajaczkowski, M. (1997) Estimation of glacial meltwater discharge into Svalbard coastal waters. *Oceanologia* **39**.

Beszczynska-Möller, A. and Wisotzki, A. (2012) Physical oceanography during POLARSTERN cruise ARK-XXVII/1. PANGAEA. http://dx.doi.org/10.1594/PANGAEA.801791

Bignami, F. and Hopkins, T.S. (1997) The water mass characteristics of the Northeast Water Polynya: Polar Sea data 1992-1993. *Journal of Marine Systems* **10**, 139-156. http://dx.doi.org/10.1016/S0924-7963(96)00079-6

Bourke, R.H., Newton, J.L., Paquette, R.G. and Tunnicliffe, M.D. (1987) Circulation and Water Masses of the East-Greenland Shelf. *J Geophys Res-Oceans* **92**, 6729-6740. http://dx.doi.org/10.1029/JC092iC07p06729

Budéus, G. and Schneider, W. (1995) On the hydrography of the Northeast Water Polynya. *J Geophys Res-Oceans* **100**, 4287-4299. http://dx.doi.org/10.1029/94JC02024

Budéus, G., Schneider, W. and Kattner, G. (1997) Distribution and exchange of water masses in the Northeast Water polynya (Greenland Sea). *Journal of Marine Systems* **10**, 123-138. http://dx.doi.org/10.1016/s0924-7963(96)00074-7

Chen, T.Y., Stumpf, R., Frank, M., Beldowski, J. and Staubwasser, M. (2013) Contrasting geochemical cycling of hafnium and neodymium in the central Baltic Sea. *Geochimica Et Cosmochimica Acta* **123**, 166-180. http://dx.doi.org/10.1016/j.gca.2013.09.011

Craig, H. (1961) Isotopic Variations in Meteoric Waters. *Science* **133**, 1702-1703. http://dx.doi.org/10.1126/science.133.3465.1702

Dahlqvist, R., Andersson, P.S. and Porcelli, D. (2007) Nd isotopes in Bering Strait and Chukchi Sea Water. *Geochim. Cosmochim. Acta* **71**, A196.

de Steur, L., Hansen, E., Mauritzen, C., Beszczynska-Möller, A. and Fahrbach, E. (2014) Impact of recirculation on the East Greenland Current in Fram Strait: Results from moored current meter measurements between 1997 and 2009. *Deep Sea Research Part I: Oceanographic Research Papers* **92**, 26-40. http://dx.doi.org/10.1016/j.dsr.2014.05.018

de Steur, L., Pickart, R.S., Torres, D.J. and Valdimarsson, H. (2015) Recent changes in the freshwater composition east of Greenland. *Geophysical Research Letters* **42**, 2326-2332. http://dx.doi.org/10.1002/2014gl062759

Dodd, P.A., Heywood, K.J., Meredith, M.P., Naveira-Garabato, A.C., Marca, A.D. and Falkner, K.K. (2009) Sources and fate of freshwater exported in the East Greenland

Current. *Geophysical Research Letters* **36**. http://dx.doi.org/10.1029/2009gl039663

Dodd, P.A., Rabe, B., Hansen, E., Falck, E., Mackensen, A., Rohling, E., Stedmon, C. and Kristiansen, S. (2012) The freshwater composition of the Fram Strait outflow derived from a decade of tracer measurements. *J Geophys Res-Oceans* **117**. http://dx.doi.org/10.1029/2012jc008011

Ekwurzel, B., Schlosser, P., Mortlock, R.A., Fairbanks, R.G. and Swift, J.H. (2001) River runoff, sea ice meltwater, and Pacific water distribution and mean residence times in the Arctic Ocean. *J Geophys Res-Oceans* **106**, 9075-9092. http://dx.doi.org/10.1029/1999jc000024

Epstein, S. and Mayeda, T. (1953) Variation of O-18 Content of Waters from Natural Sources. *Geochimica Et Cosmochimica Acta* **4**, 213-224. http://dx.doi.org/10.1016/0016-7037(53)90051-9

Falck, E. (2001) Contribution of waters of Atlantic and Pacific origin in the Northeast Water Polynya. *Polar Research* **20**, 193-200. http://dx.doi.org/10.1111/j.1751-8369.2001.tb00056.x

Falck, E., Kattner, G. and Budeus, G. (2005) Disappearance of Pacific Water in the northwestern Fram Strait. *Geophysical Research Letters* **32**. http://dx.doi.org/10.1029/2005gl023400

Fernández-Méndez, M., Katlein, C., Rabe, B., Nicolaus, M., Peeken, I., Bakker, K., Flores, H. and Boetius, A. (2015) Photosynthetic production in the central Arctic Ocean during the record sea-ice minimum in 2012. *Biogeosciences* **12**, 3525-3549. http://dx.doi.org/10.5194/bg-12-3525-2015

Frank, M. (2002) Radiogenic isotopes: Tracers of past ocean circulation and erosional input. *Reviews of Geophysics* **40**. http://dx.doi.org/10.1029/2000rg000094

Garcia-Solsona, E., Jeandel, C., Labatut, M., Lacan, F., Vance, D., Chavagnac, V. and Pradoux, C. (2014) Rare earth elements and Nd isotopes tracing water mass mixing and particle-seawater interactions in the SE Atlantic. *Geochimica Et Cosmochimica Acta* **125**, 351-372. http://dx.doi.org/10.1016/j.gca.2013.10.009

Gascard, J.C., Raisbeck, G., Sequeira, S., Yiou, F. and Mork, K.A. (2004) The Norwegian Atlantic Current in the Lofoten basin inferred from hydrological and tracer data (129I) and its interaction with the Norwegian Coastal Current. *Geophysical Research Letters* **31**. http://dx.doi.org/10.1029/2003gl018303

Goldstein, S.L. and Hemming, S.R. (2003) Long-lived Isotopic Tracers in Oceanography, Paleoceanography, and Ice-sheet Dynamics. *Treatise on geochemistry* **6**, 453-489. http://dx.doi.org/10.1016/B0-08-043751-6/06179-X

Grasshoff, K., Kremling, K. and Ehrhardt, M. (2009) Methods of seawater analysis. John Wiley & Sons. http://dx.doi.org/10.1002/9783527613984

Haley, B.A., Frank, M., Hathorne, E.C. and Pisias, N. (2014) Biogeochemical implications from dissolved rare earth element and Nd isotope distributions in the Gulf of Alaska. *Geochimica Et Cosmochimica Acta* **126**, 455-474. http://dx.doi.org/10.1016/j.gca.2013.11.012

Hansen, B. and Østerhus, S. (2000) North Atlantic–Nordic Seas exchanges. *Progress in Oceanography* **45**, 109-208. http://dx.doi.org/10.1016/s0079-6611(99)00052-x

Hathorne, E.C., Haley, B.A., Stichel, T., Grasse, P., Zieringer, M. and Frank, M. (2012) Online preconcentration ICP-MS analysis of rare earth elements in seawater. *Geochemistry, Geophysics, Geosystems* **13**, n/a-n/a. http://dx.doi.org/10.1029/2011gc003907

Hathorne, E.C., Stichel, T., Bruck, B. and Frank, M. (2015) Rare earth element distribution in the Atlantic sector of the Southern Ocean: The balance between particle scavenging and vertical supply. *Marine Chemistry* **177**, 157-171. http://dx.doi.org/10.1016/j.marchem.2015.03.011

Hattermann, T., Isachsen, P.E., von Appen, W.-J., Albretsen, J. and Sundfjord, A. (2016) Eddy-driven recirculation of Atlantic Water in Fram Strait. *Geophysical Research Letters* **43**, 3406-3414. http://dx.doi.org/10.1002/2016gl068323

Hopwood, M.J., Bacon, S., Arendt, K., Connelly, D.P. and Statham, P.J. (2015) Glacial meltwater from Greenland is not likely to be an important source of Fe to the North Atlantic. *Biogeochemistry* **124**, 1-11. http://dx.doi.org/10.1007/s10533-015-0091-6

47

Jacobsen, S.B. and Wasserburg, G.J. (1980) Sm-Nd Isotopic Evolution of Chondrites. *Earth and Planetary Science Letters* **50**, 139-155. http://dx.doi.org/10.1016/0012-821x(80)90125-9

Jakobsson, M., Mayer, L., Coakley, B., Dowdeswell, J.A., Forbes, S., Fridman, B., Hodnesdal, H., Noormets, R., Pedersen, R., Rebesco, M., Schenke, H.W., Zarayskaya, Y., Accettella, D., Armstrong, A., Anderson, R.M., Bienhoff, P., Camerlenghi, A., Church, I., Edwards, M., Gardner, J.V., Hall, J.K., Hell, B., Hestvik, O., Kristoffersen, Y., Marcussen, C., Mohammad, R., Mosher, D., Nghiem, S.V., Pedrosa, M.T., Travaglini, P.G. and Weatherall, P. (2012) The International Bathymetric Chart of the Arctic Ocean (IBCAO) Version 3.0. *Geophysical Research Letters* **39**. http://dx.doi.org/10.1029/2012gl052219

Jeandel, C. and Oelkers, E.H. (2015) The influence of terrigenous particulate material dissolution on ocean chemistry and global element cycles. *Chemical Geology* **395**, 50-66. http://dx.doi.org/10.1016/j.chemgeo.2014.12.001

Jones, E.P. and Anderson, L.G. (1986) On the Origin of the Chemical-Properties of the Arctic-Ocean Halocline. *J Geophys Res-Oceans* **91**, 759-767. http://dx.doi.org/10.1029/JC091iC09p10759

Jones, E.P., Anderson, L.G., Jutterstrom, S., Mintrop, L. and Swift, J.H. (2008a) Pacific freshwater, river water and sea ice meltwater across Arctic Ocean basins: Results from the 2005 Beringia Expedition. *J Geophys Res-Oceans* **113**. http://dx.doi.org/10.1029/2007jc004124

Jones, E.P., Anderson, L.G., Jutterstrom, S. and Swift, J.H. (2008b) Sources and distribution of fresh water in the East Greenland Current. *Progress in Oceanography* **78**, 37-44. http://dx.doi.org/10.1016/j.pocean.2007.06.003

Jones, E.P., Anderson, L.G. and Swift, J.H. (1998) Distribution of Atlantic and Pacific waters in the upper Arctic Ocean: Implications for circulation. *Geophysical Research Letters* **25**, 765-768. http://dx.doi.org/10.1029/98gl00464

Lacan, F. (2002) Masses d'eau des Mers Nordiques et de l'Atlantique Subarctique tracées par les isotopes du néodyme. Université Paul Sabatier-Toulouse III.

Lacan, F. and Jeandel, C. (2001) Tracing Papua New Guinea imprint on the central Equatorial Pacific Ocean using neodymium isotopic compositions and Rare Earth Element patterns. *Earth and Planetary Science Letters* **186**, 497-512. http://dx.doi.org/10.1016/S0012-821x(01)00263-1

Lacan, F. and Jeandel, C. (2004a) Denmark Strait water circulation traced by heterogeneity in neodymium isotopic compositions. *Deep-Sea Research Part I-Oceanographic Research Papers* **51**, 71-82. http://dx.doi.org/10.1016/j.dsr.2003.09.006

Lacan, F. and Jeandel, C. (2004b) Neodymium isotopic composition and rare earth element concentrations in the deep and intermediate Nordic Seas: Constraints on the Iceland Scotland Overflow Water signature. *Geochemistry Geophysics Geosystems* **5**. http://dx.doi.org/10.1029/2004gc000742

Lacan, F. and Jeandel, C. (2005) Neodymium isotopes as a new tool for quantifying exchange fluxes at the continent–ocean interface. *Earth and Planetary Science Letters* **232**, 245-257. http://dx.doi.org/10.1016/j.epsl.2005.01.004

Lambelet, M., van de Flierdt, T., Crocket, K., Rehkamper, M., Kreissig, K., Coles, B., Rijkenberg, M.J.A., Gerringa, L.J.A., de Baar, H.J.W. and Steinfeldt, R. (2016) Neodymium isotopic composition and concentration in the western North Atlantic Ocean: Results from the GEOTRACES GA02 section. *Geochimica Et Cosmochimica Acta* **177**, 1-29. http://dx.doi.org/10.1016/j.gca.2015.12.019

Le Fèvre, B. and Pin, C. (2005) A straightforward separation scheme for concomitant Lu–Hf and Sm–Nd isotope ratio and isotope dilution analysis. *Analytica Chimica Acta* **543**, 209-221. http://dx.doi.org/10.1016/j.aca.2005.04.044

Loeng, H. (1991) Features of the Physical Oceanographic Conditions of the Barents Sea. *Polar Research* **10**, 5-18. http://dx.doi.org/10.1111/j.1751-8369.1991.tb00630.x

Marnela, M., Rudels, B., Houssais, M.N., Beszczynska-Möller, A. and Eriksson, P.B. (2013) Recirculation in the Fram Strait and transports of water in and north of the Fram Strait derived from CTD data. *Ocean Science* **9**, 499-519. http://dx.doi.org/10.5194/os-9-499-2013

McLennan, S.M. (2001) Relationships between the trace element composition of sedimentary rocks and upper continental crust. *Geochemistry Geophysics Geosystems* **2**. http://dx.doi.org/10.1029/2000GC000109

Molina-Kescher, M., Frank, M. and Hathorne, E.C. (2014) South Pacific dissolved Nd isotope compositions and rare earth element distributions: Water mass mixing versus biogeochemical cycling. *Geochimica Et Cosmochimica Acta* **127**, 171-189. http://dx.doi.org/10.1016/j.gca.2013.11.038

Newton, R., Schlosser, P., Mortlock, R., Swift, J. and MacDonald, R. (2013) Canadian Basin freshwater sources and changes: Results from the 2005 Arctic Ocean Section. *J Geophys Res-Oceans* **118**, 2133-2154. http://dx.doi.org/10.1002/jgrc.20101

Osborne, A.H., Haley, B.A., Hathorne, E.C., Plancherel, Y. and Frank, M. (2015) Rare earth element distribution in Caribbean seawater: Continental inputs versus lateral transport of distinct REE compositions in subsurface water masses. *Marine Chemistry* **177**, 172-183. http://dx.doi.org/10.1016/j.marchem.2015.03.013

Persson, P.O., Andersson, P.S., Porcelli, D. and Semiletov, I. (2011) The influence of Lena River water inflow and shelf sediment-sea water exchange for the Nd isotopic composition in the Laptev Sea and Arctic Ocean. *Geophysical Research Abstracts* **13**.

Petrova, M. (2015) Neodymium isotopes and rare earth element distribution in the Barents Sea, Arctic Ocean. *Master thesis, Saint Petersburg State University / University of Hamburg, Saint Petersburg / Hamburg*, 60 pp.

Piepgras, D.J. and Wasserburg, G.J. (1987) Rare-Earth Element Transport in the Western North-Atlantic Inferred from Nd Isotopic Observations. *Geochimica Et Cosmochimica Acta* **51**, 1257-1271. http://dx.doi.org/10.1016/0016-7037(87)90217-1

Porcelli, D., Andersson, P.S., Baskaran, M., Frank, M., Bjork, G. and Semiletov, I. (2009) The distribution of neodymium isotopes in Arctic Ocean basins. *Geochimica Et Cosmochimica Acta* **73**, 2645-2659. http://dx.doi.org/10.1016/j.gca.2008.11.046

Rabe, B., Dodd, P.A., Hansen, E., Falck, E., Schauer, U., Mackensen, A., Beszczynska-Möller, A., Kattner, G., Rohling, E.J. and Cox, K. (2013) Liquid export of Arctic freshwater components through the Fram Strait 1998-2011. *Ocean Science* **9**, 91-109. http://dx.doi.org/10.5194/os-9-91-2013

Rabe, B., Schauer, U., Mackensen, A., Karcher, M., Hansen, E. and Beszczynska-Möller, A. (2009) Freshwater components and transports in the Fram Strait - recent observations and changes since the late 1990s. *Ocean Science* **5**, 219-233. http://dx.doi.org/10.5194/os-5-219-2009

Rempfer, J., Stocker, T.F., Joos, F., Dutay, J.C. and Siddall, M. (2011) Modelling Nd-isotopes with a coarse resolution ocean circulation model: Sensitivities to model parameters and source/sink distributions. *Geochimica Et Cosmochimica Acta* **75**, 5927-5950. http://dx.doi.org/10.1016/j.gca.2011.07.044

Rickli, J., Frank, M. and Halliday, A.N. (2009) The hafnium-neodymium isotopic composition of Atlantic seawater. *Earth and Planetary Science Letters* **280**, 118-127. http://dx.doi.org/10.1016/j.epsl.2009.01.026

Rudels, B. (2009) Arctic Ocean Circulation. *Encyclopedia of Ocean Sciences. Elsevier*, 211-225. http://dx.doi.org/10.1016/B978-012374473-9.00601-9

Rudels, B., Anderson, L., Eriksson, P., Fahrbach, E., Jakobsson, M., Jones, E.P., Melling, H., Prinsenberg, S., Schauer, U. and Yao, T. (2012) Observations in the ocean, Arctic Climate Change. Springer, pp. 117-198. http://dx.doi.org/10.1007/978-94-007-2027-5_4

Rudels, B., Bjork, G., Nilsson, J., Winsor, P., Lake, I. and Nohr, C. (2005) The interaction between waters from the Arctic Ocean and the Nordic Seas north of Fram Strait and along the East Greenland Current: results from the Arctic Ocean-02 Oden expedition. *Journal of Marine Systems* **55**, 1-30. http://dx.doi.org/10.1016/j.jmarsys.2004.06.008

Rudels, B., Friedrich, H.J., Hainbucher, D. and Lohmann, G. (1999a) On the parameterisation of oceanic sensible heat loss to the atmosphere and to ice in an ice-covered mixed layer in winter. *Deep-Sea Research Part Ii-Topical Studies in Oceanography* **46**, 1385-1425. http://dx.doi.org/10.1016/S0967-0645(99)00028-4

Rudels, B., Friedrich, H.J. and Quadfasel, D. (1999b) The arctic circumpolar boundary current. *Deep-Sea Research Part Ii-Topical Studies in Oceanography* **46**, 1023-1062. http://dx.doi.org/10.1016/S0967-0645(99)00015-6

Rudels, B., Jones, E.P., Schauer, U. and Eriksson, P. (2004) Atlantic sources of the Arctic Ocean surface and halocline waters. *Polar Research* **23**, 181-208. http://dx.doi.org/10.1111/j.1751-8369.2004.tb00007.x

Rudels, B., Korhonen, M., Schauer, U., Pisarev, S., Rabe, B. and Wisotzki, A. (2015) Circulation and transformation of Atlantic water in the Eurasian Basin and the contribution of the Fram Strait inflow branch to the Arctic Ocean heat budget. *Progress in Oceanography* **132**, 128-152. http://dx.doi.org/10.1016/j.pocean.2014.04.003

Rudels, B., Meyer, R., Fahrbach, E., Ivanov, V.V., Østerhus, S., Quadfasel, D., Schauer, U., Tverberg, V. and Woodgate, R.A. (2000) Water mass distribution in Fram Strait and over the Yermak Plateau in summer 1997, Annales Geophysicae. Springer, pp. 687-705. http://dx.doi.org/10.1007/s00585-000-0687-5

Schlichtholz, P. and Houssais, M.-N. (2002) An overview of the teta-S correlations in Fram Strait based on the MIZEX 84 data. *Oceanologia* **44**.

Schlitzer, R. (2016) Ocean Data View. http://odv.awi.de.

Stedmon, C.A., Granskog, M.A. and Dodd, P.A. (2015) An approach to estimate the freshwater contribution from glacial melt and precipitation in East Greenland shelf waters using colored dissolved organic matter (CDOM). *J Geophys Res-Oceans* **120**, 1107-1117. http://dx.doi.org/10.1002/2014jc010501

Stichel, T., Frank, M., Rickli, J. and Haley, B.A. (2012) The hafnium and neodymium isotope composition of seawater in the Atlantic sector of the Southern Ocean. *Earth and Planetary Science Letters* **317**, 282-294. http://dx.doi.org/10.1016/j.epsl.2011.11.025

Stichel, T., Hartman, A.E., Duggan, B., Goldstein, S.L., Scher, H. and Pahnke, K. (2015) Separating biogeochemical cycling of neodymium from water mass mixing in the Eastern North Atlantic. *Earth and Planetary Science Letters* **412**, 245-260. http://dx.doi.org/10.1016/j.epsl.2014.12.008

Stöven, T., Tanhua, T., Hoppema, M. and von Appen, W.-J. (2016) Transient tracer distributions in the Fram Strait in 2012 and inferred anthropogenic carbon content and transport. *Ocean Science* **12**, 319-333. http://dx.doi.org/10.5194/os-12-319-2016

Sutherland, D.A., Pickart, R.S., Jones, E.P., Azetsu-Scott, K., Eert, A.J. and Olafsson, J. (2009) Freshwater composition of the waters off southeast Greenland and their link to the Arctic Ocean. *J Geophys Res-Oceans* **114**. http://dx.doi.org/10.1029/2008jc004808

Tachikawa, K., Athias, V. and Jeandel, C. (2003) Neodymium budget in the modern ocean and paleo-oceanographic implications. *J Geophys Res-Oceans* **108**. http://dx.doi.org/10.1029/1999jc000285

Tanaka, T., Togashi, S., Kamioka, H., Amakawa, H., Kagami, H., Hamamoto, T., Yuhara, M., Orihashi, Y., Yoneda, S., Shimizu, H., Kunimaru, T., Takahashi, K., Yanagi, T., Nakano, T., Fujimaki, H., Shinjo, R., Asahara, Y., Tanimizu, M. and Dragusanu, C. (2000) JNdi-1: a neodymium isotopic reference in consistency with LaJolla neodymium. *Chemical Geology* **168**, 279-281. http://dx.doi.org/10.1016/S0009-2541(00)00198-4

Tanhua, T., Jones, E.P., Jeansson, E., Jutterström, S., Smethie, W.M., Wallace, D.W.R. and Anderson, L.G. (2009) Ventilation of the Arctic Ocean: Mean ages and inventories of anthropogenic CO2and CFC-11. *Journal of Geophysical Research* **114**. http://dx.doi.org/10.1029/2008jc004868

Taylor, J.R., Falkner, K.K., Schauer, U. and Meredith, M. (2003) Quantitative considerations of dissolved barium as a tracer in the Arctic Ocean. *J Geophys Res-Oceans* **108**. http://dx.doi.org/10.1029/2002jc001635

Tepe, N. and Bau, M. (2015) Distribution of rare earth elements and other high field strength elements in glacial meltwaters and sediments from the western Greenland Ice Sheet: Evidence for different sources of particles and nanoparticles. *Chemical Geology* **412**, 59-68. http://dx.doi.org/10.1016/j.chemgeo.2015.07.026

Tepe, N. and Bau, M. (2016) Behavior of rare earth elements and yttrium during simulation of arctic estuarine mixing between glacial-fed river waters and seawater and the impact of inorganic (nano-)particles. *Chemical Geology* **438**, 134-145. http://dx.doi.org/10.1016/j.chemgeo.2016.06.001

Top, Z., Bignami, F. and Hopkins, T. (1997) Tritium-3He ages of deep waters in the NEW Polynya. *Journal of Marine Systems* **10**, 175-184. http://dx.doi.org/10.1016/s0924-7963(96)00064-4

van de Flierdt, T., Pahnke, K., Amakawa, H., Andersson, P.S., Basak, C., Coles, B., Colin, C., Crocket, K., Frank, M., Frank, N., Goldstein, S.L., Goswami, V., Haley, B.A., Hathorne, E.C., Hemming, S.R., Henderson, G.M., Jeandel, C., Jones, K., Kreissig, K., Lacan, F., Lambelet, M., Martin, E.E., Newkirk, D.R., Obata, H., Pena, L., Piotrowski, A.M., Pradoux, C., Scher, H.D., Schöberg, H., Singh, S.K., Stichel, T., Tazoe, H., Vance, D. and Yang, J. (2012) GEOTRACES intercalibration of neodymium isotopes and rare earth element concentrations in seawater and suspended particles. Part 1: reproducibility of results for the international intercomparison. *Limnology and Oceanography: Methods* **10**, 234-251. http://dx.doi.org/10.4319/lom.2012.10.234

von Appen, W.-J., Schauer, U., Hattermann, T. and Beszczynska-Möller, A. (2016) Seasonal Cycle of Mesoscale Instability of the West Spitsbergen Current. *Journal of Physical Oceanography* **46**, 1231-1254. http://dx.doi.org/10.1175/jpo-d-15-0184.1

von Appen, W.-J., Schauer, U., Somavilla, R., Bauerfeind, E. and Beszczynska-Möller, A. (2015) Exchange of warming deep waters across Fram Strait. *Deep Sea Research Part I: Oceanographic Research Papers* **103**, 86-100. http://dx.doi.org/10.1016/j.dsr.2015.06.003

Walczowski, W. (2013) Frontal structures in the West Spitsbergen Current margins. *Ocean Science* **9**, 957-975. http://dx.doi.org/10.5194/os-9-957-2013

Walczowski, W., Piechura, J., Osinski, R. and Wieczorek, P. (2005) The West Spitsbergen Current volume and heat transport from synoptic observations in summer. *Deep-Sea Research Part I-Oceanographic Research Papers* **52**, 1374-1391. http://dx.doi.org/10.1016/j.dsr.2005.03.009

Werner, K., Frank, M., Teschner, C., Muller, J. and Spielhagen, R.F. (2014) Neoglacial change in deep water exchange and increase of sea-ice transport through eastern Fram Strait: evidence from radiogenic isotopes. *Quaternary Science Reviews* **92**, 190-207. http://dx.doi.org/10.1016/j.quascirev.2013.06.015

Westerlund, S. and Ohman, P. (1992) Rare earth elements in the Arctic Ocean. *Deep-Sea Research Part a-Oceanographic Research Papers* **39**, 1613-1626. http://dx.doi.org/10.1016/0198-0149(92)90051-T

Woodgate, R.A., Fahrbach, E. and Rohardt, G. (1999) Structure and transports of the East Greenland Current at 75 degrees N from moored current meters. *J Geophys Res-Oceans* **104**, 18059-18072. http://dx.doi.org/10.1029/1999jc900146

Yamamoto-Kawai, M., McLaughlin, F.A., Carmack, E.C., Nishino, S. and Shimada, K. (2008) Freshwater budget of the Canada Basin, Arctic Ocean, from salinity, δ18O, and nutrients. *Journal of Geophysical Research* **113**. http://dx.doi.org/10.1029/2006jc003858

Yang, J. and Haley, B. (2016) The profile of the rare earth elements in the Canada Basin, Arctic Ocean. *Geochemistry, Geophysics, Geosystems* **17**, 3241-3253. http://dx.doi.org/10.1002/2016gc006412

Zimmermann, B., Porcelli, D., Frank, M., Andersson, P.S., Baskaran, M., Lee, D.C. and Halliday, A.N. (2009) Hafnium isotopes in Arctic Ocean water. *Geochimica Et Cosmochimica Acta* **73**, 3218-3233. http://dx.doi.org/10.1016/j.gca.2009.02.028

Table 1

REE sources in the Arctic Mediterranean	Abbreviation	salinity	ε_{Nd}	ε_{Nd} 1SD*/n**	[Nd] (pmol/kg)
Atlantic Water at the Iceland-Scotland Ridge	AW-ISR	35.27	-13.0	0.6/7	16.2
Atlantic Water at the Denmark Strait	AW-DS	35.10	-12.6	0.8/2	19.1
Pacific Water emerging from Chuckchi Sea	PACW	32.70	-5.5	-	30.0
Norwegian Coastal Water in the western Barents Sea	NCW	34.52	-14.5	0.4/2	22.5
Ob River freshwater	Ob	0	-6.1	0.3/1	2152
Lena River freshwater	Lena	0	-15 to -15.7	>0.2/2	~600
Yenisei River freshwater	Yenisei	0	-5.2	0.3/1	154
Kolyma River freshwater	Kolyma	0	-6.0	0.4/1	129
Mackenzie River freshwater	Mackenzie	0	-12.9	0.3/1	111

Water mass compositions - Fram Strait (summer 2012)	Abbreviation	salinity	ε_{Nd}	ε_{Nd} 1SD*/n**	[Nd] (pmol/kg)
Atlantic-derived waters					
Atlantic Water	AW	35.09	-11.7	0.4/11	15.9
Recirculating Atlantic Water	RAW	35.01	-11.6	0.1/3	16.3
dense Arctic Atlantic Water	dAAW	34.91	-10.4	0.2/5	16.3
Arctic-derived waters					
Polar Water (most radiogenic sample)	PWεNd-max	32.30	-8.8	0.2/1	26.3
Polar Water (all samples)	PW	33.01	-9.9	0.7/7	27.1
Knee Water	KW	33.98	-9.6	0.2/3	22.3
Locally modified waters					
NE Greenland Shelf Shallow Water	NEGSSW	31.41	-11.7	0.5/13	36.6
NE Greenland Shelf Bottom Water	NEGSBW	34.28	-11.8	0.2/4	24.0
Intermediate and deep waters					
Arctic Intermediate Water	AIW	34.91	-10.1	0.2/4	15.5
Upper Polar Deep Water	UPDW	34.90	-10.2	0.4/5	15.7
Nordic Seas Deep Water	NDW	34.91	-10.0	0.2/3	16.1
Eurasian Basin Deep Water / Greenland Sea Deep Water	EBDW/GSDW	34.92	-10.5	0.2/6	15.8
Canadian Basin Deep Water	CBDW	34.92	-10.1	0.5/3	15.4

* standard deviation of sample mean; the measurement uncertainty (2 SD) is shown instead if 1 SD of mean is zero or only one sample

** number of samples used to calculate ε_{Nd} mean

Table 1 PDF

REE sources in the Arctic Mediterranean	Abbreviation	salinity	ε_{Nd}	ε_{Nd} 1SD*/n**	[Nd] (pmol/kg)	Reference
Atlantic Water at the Iceland-Scotland Ridge	AW-ISR	35.27	-13.0	0.6/7	16.2	Lacan & Jeandel (2004b)
Atlantic Water at the Denmark Strait	AW-DS	35.10	-12.6	0.8/2	19.1	Lacan & Jeandel (2004a)
Pacific Water emerging from Chuckchi Sea	PACW	32.70	-5.5	-	30.0	Porcelli et al. (2009), Dahlqvist et al. (2007)
Norwegian Coastal Water in the western Barents Sea	NCW	34.52	-14.5	0.4/2	22.5	Petrova (2015)
Ob River freshwater	Ob	0	-6.1	0.3/1	2152	Zimmermann et al. (2009)
Lena River freshwater	Lena	0	-15 to -15.7	>0.2/2	~600	Persson et al. (2011), this study
Yenisei River freshwater	Yenisei	0	-5.2	0.3/1	154	Zimmermann et al. (2009)
Kolyma River freshwater	Kolyma	0	-6.0	0.4/1	129	Porcelli et al. (2009)
Mackenzie River freshwater	Mackenzie	0	-12.9	0.3/1	111	Zimmermann et al. (2009)

Water mass compositions - Fram Strait (summer 2012)	Abbreviation	salinity	ε_{Nd}	ε_{Nd} 1SD*/n**	[Nd] (pmol/kg)
Atlantic-derived waters					
Atlantic Water	AW	35.09	-11.7	0.4/11	15.9
Recirculating Atlantic Water	RAW	35.01	-11.6	0.1/3	16.3
dense Arctic Atlantic Water	dAAW	34.91	-10.4	0.2/5	16.3
Arctic-derived waters					
Polar Water (most radiogenic sample)	PWεNd-max	32.30	-8.8	0.2/1	26.3
Polar Water (all samples)	PW	33.01	-9.9	0.7/7	27.1
Knee Water	KW	33.98	-9.6	0.2/3	22.3
Locally modified waters					
NE Greenland Shelf Shallow Water	NEGSSW	31.41	-11.7	0.5/13	36.6
NE Greenland Shelf Bottom Water	NEGSBW	34.28	-11.8	0.2/4	24.0
Intermediate and deep waters					
Arctic Intermediate Water	AIW	34.91	-10.1	0.2/4	15.5
Upper Polar Deep Water	UPDW	34.90	-10.2	0.4/5	15.7
Nordic Seas Deep Water	NDW	34.91	-10.0	0.2/3	16.1
Eurasian Basin Deep Water / Greenland Sea Deep Water	EBDW/GSDW	34.92	-10.5	0.2/6	15.8
Canadian Basin Deep Water	CBDW	34.92	-10.1	0.5/3	15.4

* standard deviation of sample mean; the measurement uncertainty (2 SD) is shown instead if 1 SD of mean is zero or only one sample was used

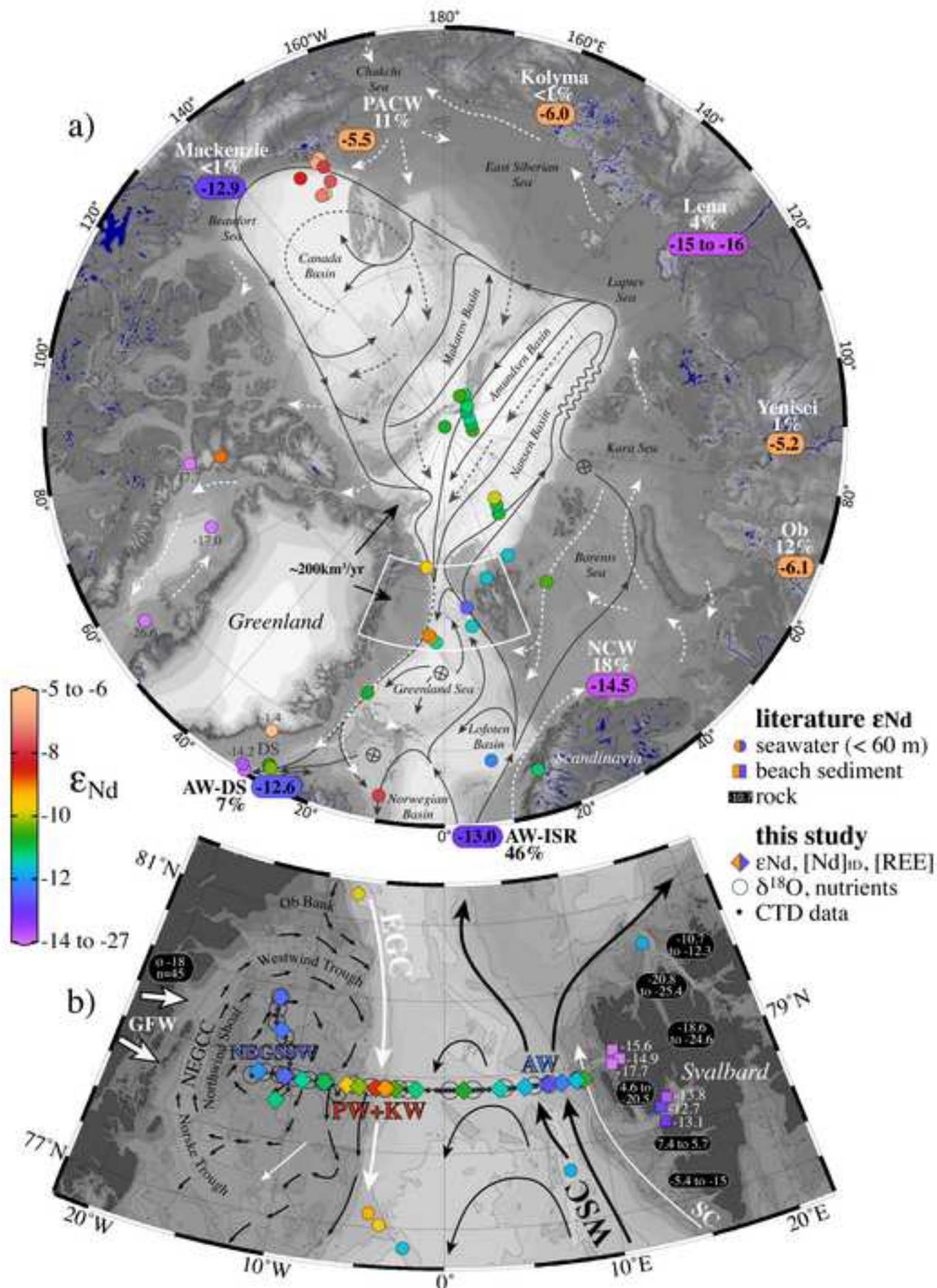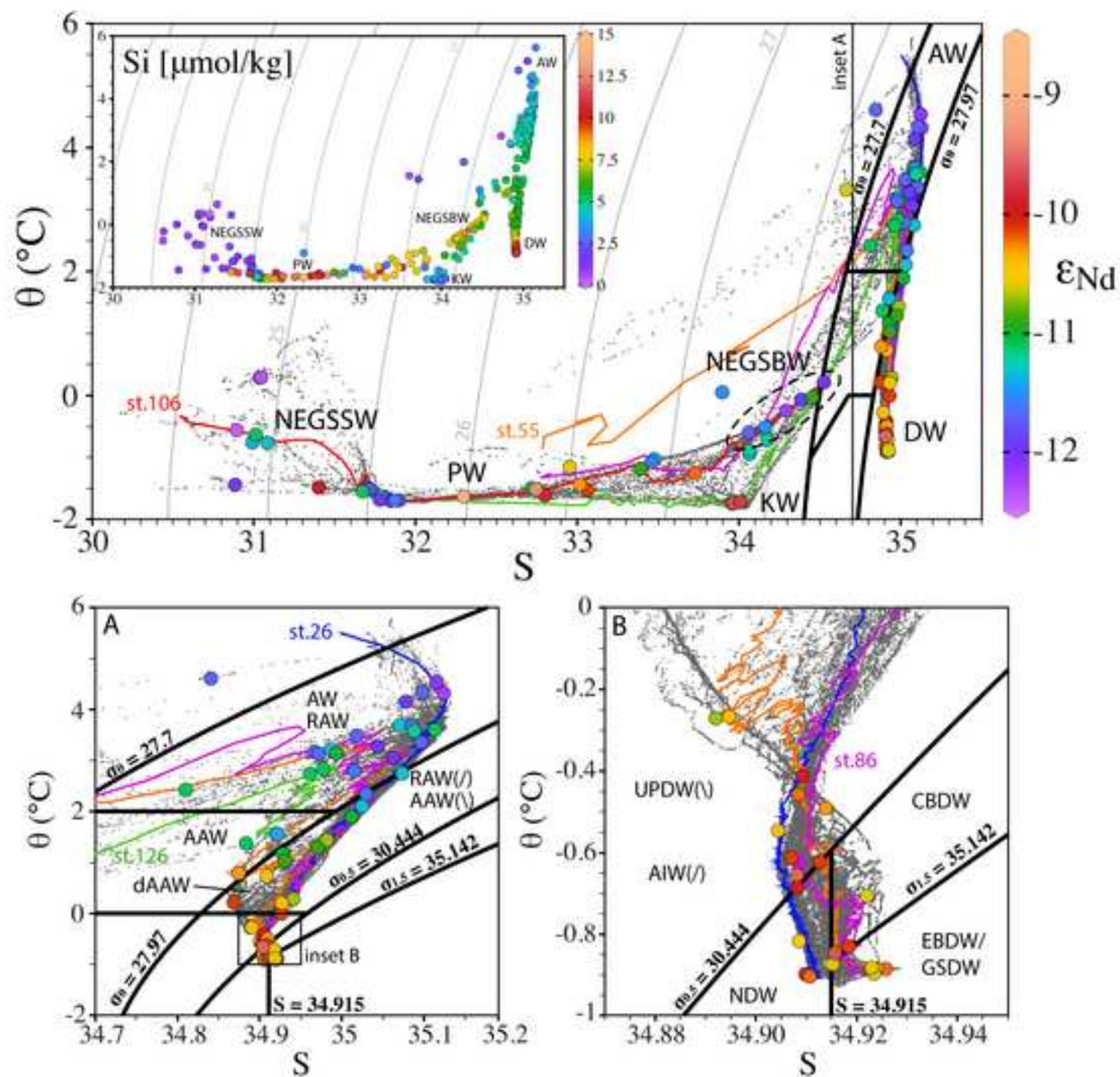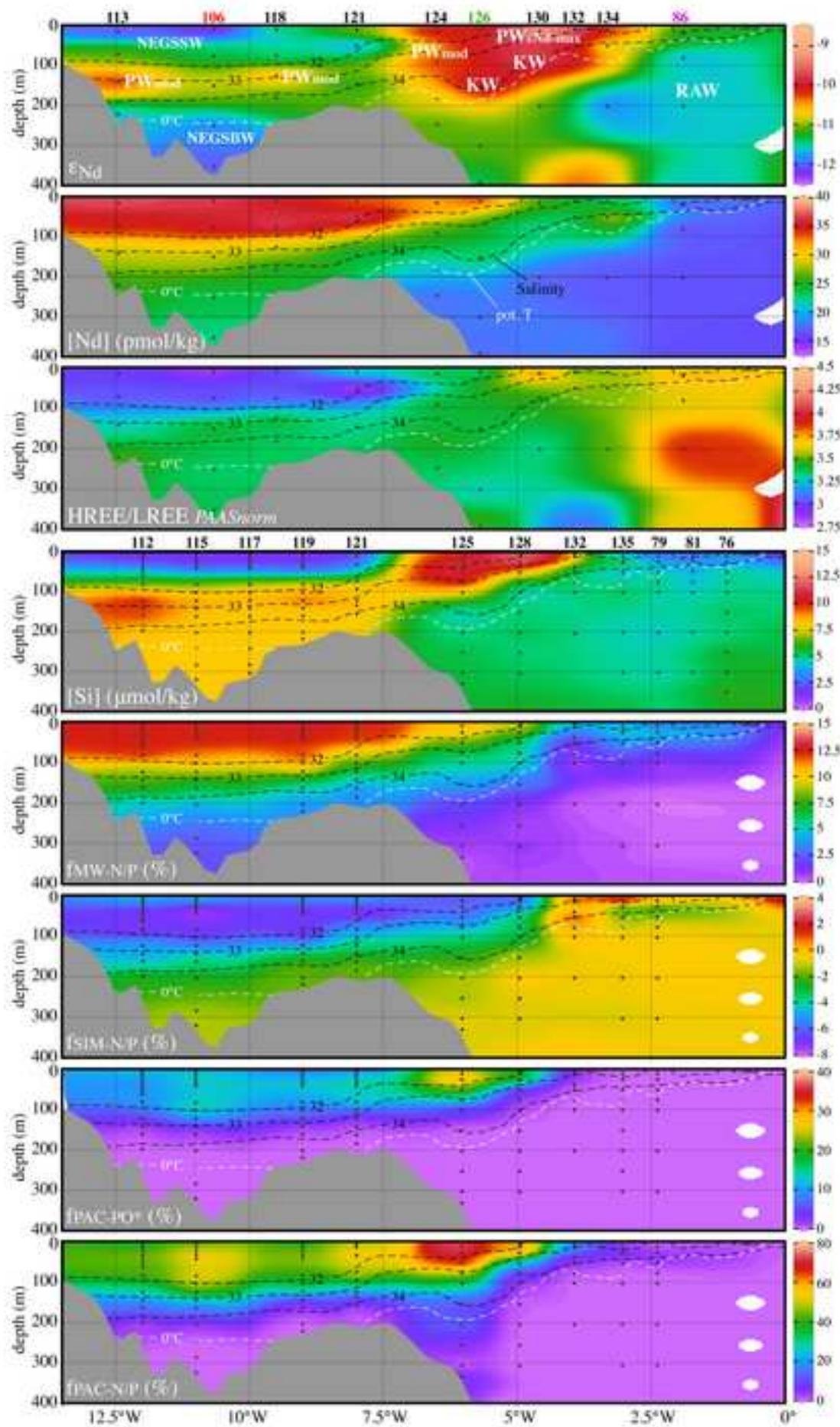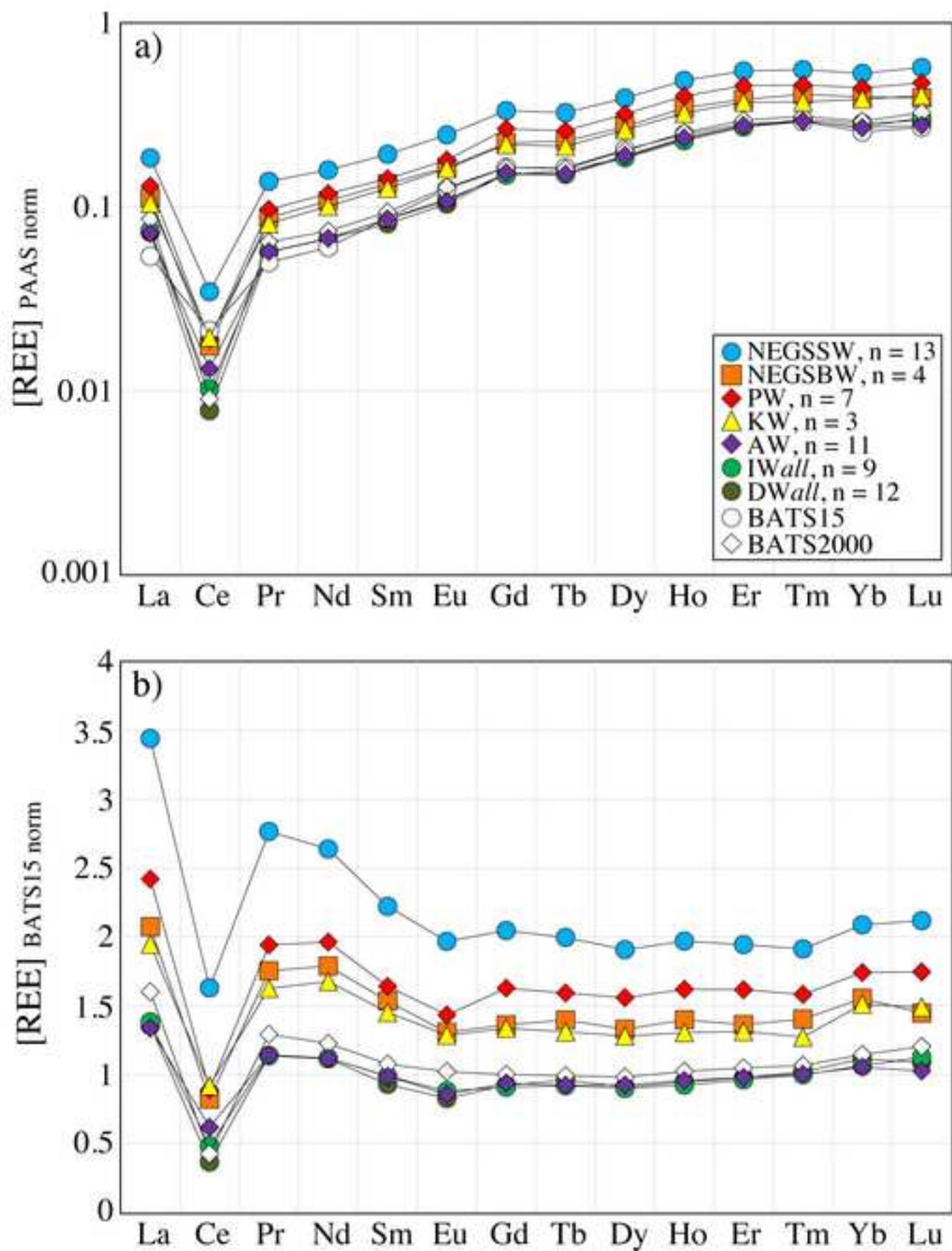** number of samples used to calculate ε_{Nd} mean

Figure 1

Figure 2

Figure 3

Figure 4

Figure 5

Figure 6

Figure 7

Atlantic Layer

◆ Iceland-Scotland Ridge, 1999, n = 7
◆ Denmark Strait, 1999, n = 2
◆ eastern Norwegian Sea &
  Lofoten Basin, 1999, n = 2
△ western Barents Sea, 2014, n = 5
▲ Fram Strait, 2012, n = 11
▲ Fram Strait, 2011, n = 1
● north of Svalbard, 2001, n = 2
● Nansen Basin, 2001, n = 3
● Amundsen Basin, 2001, n = 3
● Laptev Sea margin, 2014, n = 1
● Makarov Basin, 2001, n = 2
● Canada Basin, 2000, n = 3

■ RAW, Fram Strait 2012, n = 3
■ dAAW, Fram Strait 2012, n = 5

Intermediate Layer

Whole AM, 1999-2012, n = 22
Iceland & Norwegian Seas, 1999, n = 2

Figure 8

Figure 9